Tectonic evolution of high-grade metamorphic tectonites of the Meelpaeg structure near Port aux Basques, southwestern Newfoundland during the Silurian Salinic and Early-to-Middle Devonian Acadian orogenies

C. R. van Staal [a,b], S. Lin[b], P. Valverde-Vaquero[c], G. Dunning[d], J. Burgess[e], D. Schofield[f], and N. Joyce[g]

[a]Geological Survey of Canada, Vancouver, BC, V6B 5J3, Canada; [b]University of Waterloo, Waterloo, ON, N2L 3G1, Canada; [c]Instituto Geológico y Minero de España, La Calera 1, Tres Cantos, Madrid, Spain; [d]Department of Earth Sciences, Memorial University of Newfoundland, St. John's, NL A1B 3X5, Canada; [e]Johns Hopkins University, Department of Earth and Planetary Sciences, Baltimore, MD 21210, USA; [f]British Geological Survey, the Lyell Centre, Research Avenue South, Edinburgh EH14 4AP, UK; [g]Geological Survey of Canada, Ottawa, ON K1A 0E8, Canada

Corresponding author: **C. R. van Staal** (email: cees.vanstaal@NRcan-RNcan.gc.ca)

Abstract

The Meelpaeg structure in southwestern Newfoundland comprises allochthonous tectonites formed during the Salinic (D_{1-2}) and Acadian (D_3) orogenies. D_{1-2} occurred between 451 and 417 Ma and culminated in Barrovian metamorphism during terminal collision of the Gander margin with composite Laurentia. Collision was followed by tectonic escape of the deeply buried rocks between 417 and 412 Ma. Rocks of the Victoria arc and Exploits backarc preserved in the Port aux Basques and Grand Bay complexes were emplaced during D_1 by the Grandys River shear zone, which is outlined by a narrow band of the ca. 451 Ma Port aux Basques granite, towards the southeast above the Harbour le Cou Group. The contrasting histories displayed across the Grandys River shear zone are typical of the Dog Bay Line further northeast. Salinic structures were overprinted by faults and folds formed during Acadian D_3 transpression ($\leq$412 Ma), which produced the bi-vergent Meelpaeg structure and emplacement of amphibolite facies tectonites above greenschist facies rocks along its bounding shear zones. F_3 folding progressively steepened the faults, which in turn led to progressive localization of dextral strike–slip in narrow fault zones. The high grade of metamorphism in the Meelpaeg structure is attributed to protracted underthrusting of the Cabot promontory of the Gander margin beneath composite Laurentia. Salinic convergence was sinistral but became dextral during the Early Devonian, diachronous Acadian orogeny. The kinematic switch is proposed as a tool to separate Salinic from Acadian structures in the central part of the northern Appalachians.

Key words: Newfoundland, Salinic, Acadian, tectonic escape, switch in oblique convergence, transpression

Introduction

The regional extent, duration, and tectonic significance of the Silurian Salinic orogeny have remained contentious issues since its recognition following detailed geochronological studies in the polyorogenic core of the northern Appalachians (e.g., Dunning et al. 1990). Salinic orogenesis was attributed to the Late Ordovician to Silurian sinistral oblique closure of a Middle Ordovician backarc basin, which formed in Ganderia due to arc rifting and backarc spreading during its convergence with Laurentia (van Staal 1994; van Staal et al. 1998, 2012, 2016; Valverde-Vacquero et al. 2006). Backarc spreading divided Ganderia into two halves: a leading arc terrane referred to as the Popelogan–Victoria arc and a trailing margin referred to as the Gander margin (van Staal 1994). This wide oceanic backarc basin, referred to in Newfoundland as the Exploits backarc basin, rep-resents the last vestige of the Iapetus Ocean, which terminally closed during the Silurian by northwest-directed subduction (van Staal 1994). Disorganized spreading and multiple stages of arc rifting created a complex oceanic marginal basin containing several isolated ribbons of arc rocks (van Staal et al. 2003, 2016; Zagorevski et al. 2010; Fyffe et al. 2023), which sequentially accreted to composite Laurentia during its closure (van Staal et al. 2008; van Staal and Barr 2012; Wilson et al. 2015). Latest Silurian inversion of synorogenic basins such as the Fredericton–Merrimack Trough and central Maine–Matapedia belt in maritime Canada and New England (van Staal and de Roo 1995; Reusch and van Staal 2012; Dokken et al. 2018; Eusden et al. 2023) suggests that Salinic orogenesis likely occurred throughout the northern Appalachians. However, this interpretation is challenged by a lack of geochronological evidence for Silurian tectonism in

the southern New England Appalachians, which is mainly underlain by exhumed high-grade metamorphic rocks formed during the Early-to-Middle Devonian Acadian and younger orogenic events (e.g., Hillenbrand et al. 2021). The high-temperature overprint from the superimposed orogenesis thus may have destroyed most evidence for Salinic orogenesis in these rocks. The Salinic orogenic cycle ended with diachronous partial subduction (A-subduction) and structural thickening of the Gander margin, although exactly when underthrusting and tectonic processes such as slab break-off, synorogenic magmatism, and exhumation finished, is not well known (van Staal et al. 2014a). In addition, Acadian orogenesis rapidly followed and/or may have partially overlapped in time in some places with the last gasps of Salinic tectonism elsewhere (Wilson et al. 2017). The Acadian orogeny is markedly diachronous such that it becomes progressively younger from southeast to northwest (Bradley et al. 2000) and was attributed to the terminal closure of a narrow Acadian oceanic seaway between the upper plate Gander margin and lower plate Avalonia and the subsequent protracted shallow underthrusting of Avalonia beneath Ganderia (e.g., van Staal et al. 2012; van Staal and Barr 2012; Wilson et al. 2017; Bagherpur Mojaver et al. 2021). Separation of the effects of the Salinic and Acadian orogenies in metamorphic rocks on basis of time alone can therefore be difficult, which led some authors to group all post-Taconic (Ordovician) tectonism into Acadian (*sensu lato*) orogenic event (e.g., Hillenbrand et al. 2021), or proposed that Salinic and Acadian orogenies are better interpreted as one continuous orogenic cycle rather than two kinematically unrelated events (e.g., Murphy and Keppie 2005). However, separate phases of arc magmatism (Fig. 1), foreland basin development (van Staal et al. 2014a; Reusch and van Staal 2012; Wilson et al. 2017), and changes in oblique motions (e.g., O'Brien et al. 1993; Hibbard 1994; van Staal and de Roo 1995) suggest these orogenic phases represent separate events. The nature of the final phases of Salinic tectonism and the onset of Acadian orogenesis, duration of a potential hiatus, nature of oblique movements in southwestern Newfoundland, and their tectonic implications for the tectonic evolution of the northern Appalachians are topics discussed in this paper.

Geological setting of the Port aux Basques area in southwest Newfoundland

A wide belt of allochthonous, polyphase-deformed medium-to-high-pressure (8–10 Kb) amphibolite facies tectonites, previously referred to as the Port aux Basques gneiss (Brown 1976), is preserved in southwestern Newfoundland (Figs. 1 and 2) (Chorlton and Dallmeyer 1986; Owen 1992; Burgess et al. 1995). The tectonic setting and significance of the tectonites was poorly understood before detailed multidisciplinary investigations in the 1990s and 2000s (e.g., van Staal et al. 1996a, 1996b; Schofield et al. 1998; Valverde-Vaquero et al. 2000). The metamorphic tectonites near Port aux Basques are bordered by the Cape Ray Fault zone (CRFZ) in the west and the Bay le Moine fault

zone (BMFZ) in the east (Fig. 1). The CRFZ represents the Beothuk Lake Line in this part of Newfoundland, which is a new name for the Red Indian Line of Williams et al. (1988), introduced by Slack et al. (2024) following the renaming of Red Indian Lake to Beothuk Lake by the Newfoundland government, but still giving credit to the original name introduced by Williams et al. (1988). Waldron et al. (2022) referred to this line as the Mekwe'jit line. The Beothuk Lake Line is the surface expression of the boundary where different tectonostratigraphic arc assemblages formed on opposite sides of the Iapetus Ocean were structurally juxtaposed during the Late Ordovician (van Staal et al. 1998; 2007; Zagorevski et al. 2008, 2010, 2023). This boundary is referred to as a line in Newfoundland, because it is in places severely overprinted and modified by younger faults and hence not a continuous single fault (Williams et al. 1988). The southeast-dipping CRFZ (Figs. 1 and 2) is an example of a Devonian fault (Dubé et al. 1996) that significantly obscured the geometry of the structures formed during the initial, Late Ordovician juxtaposition of the two different arc terranes (Williams et al. 1988; Lin et al. 1994; Valverde-Vaquero et al. 2006). Seismic and geological evidence indicate that the original fault zone and associated structures that marked the Beothuk Lake Line had a dip to the northwest due to subduction of the Godwanan Victoria arc and its older Penobscot arc substrate beneath the peri-Laurentian arc terrane (Thurlow et al. 1992; Zagorevski et al. 2008, 2010). The older northwest-dipping fault segment of the Beothuk Lake Line and the adjacent rocks of the Victoria arc in central Newfoundland are truncated and overridden to the southwest by the southeast-dipping Victoria Lake shear zone (Fig. 1) (Valverde-Vaquero et al. 2006), which is the along strike continuation of the CRFZ to the northeast after restoring the dextral transcurrent motion along the intervening Gunflap Hills fault (Fig. 1) (Lin et al. 1994). Together the CRFZ and the Victoria Lake shear zone represent the western-leading basal thrust of the Acadian "Meelpaeg nappe" (Fig. 1) of Valverde-Vaquero et al. (2006), which was defined by the structural emplacement of high-grade metamorphic tectonites and associated granitoid bodies above lower grade (greenschist facies) rocks on all sides. Part of the Victoria arc and any older substrate are therefore probably structurally buried beneath the western part of the "Meelpaeg nappe," because the southeast-dipping CRFZ and the Victoria Lake shear zone accommodated major westward-directed thrusting during the Devonian (Dubé et al. 1996). Sructural evidence is presented herein that the "Meelpaeg nappe" is not a single thrust nappe, but an allochthonous belt of metamorphic tectonites, referred to herein as the Meelpaeg structure and the Meelpaeg tectonites. The Meelpaeg structure (Figs. 1 and 2) is bordered by two opposite verging thrust faults (CRFZ and BMFZ), which in part are interpreted to have been active at different times and accommodated different kinematic evolutions. Reference to the "Meelpaeg nappe" where used is therefore given in quotation marks. The allochthonous Meelpaeg structure terminates in central Newfoundland, although the nature of the structural termination is obscured by intrusion of a large Middle Devonian granite (ca. 386 Ma) (Valverde-Vaquero et al. 2006). Movement on the bordering

Fig. 1. Geology of southern Newfoundland with inset showing the area of the map and realm and zonal divisions of Newfoundland modified from Hibbard et al. (2006) and van Staal et al. (2014*a*); tectonic settings of the zones after. Names of plutons, units, major faults, and outline of Meelpaeg structure in black, whereas geographic locations are in light grey. Barc, backarc; ba-margin, backarc basin passive margin; BF, Billiards Brook Formation; BDFZ, Bay d'Est Fault Zone; BDNG, Bay du Nord Group; BEG, Bay d'Espoir Group; BHG, Baggs Hill Granite; BLL, Beothuk Lake Line; BMFZ, Bay le Moine Fault Zone; BVBL, Baie Verte Brompton Line; BVOT, Baie Verte Oceanic Tract; CF, Cabot Fault; CRFZ, Cape Ray Fault Zone; DBL, Dog Bay Line; DCF, Day Cove Fault; DF, Dover Fault; Exbarc, Exploits backarc; GBFZ, Grand Bay Fault Zone; GHF, Gunflap Hills Fault; GRSZ, Grandys River Shear Zone; HBF, Hermitage Bay Fault; IIG forlandbas, Indian Island Group foreland basin; IMF, Isle aux Mort Fault; LPG, La Poile Granite; LPGP, La Poile Group; MS, Meelpaeg structure; RBG, Rose blanche Granite; RRB, Rocky Ridge Belt: Varc, Victoria arc; VLSZ, Victoria Lake Shear Zone.
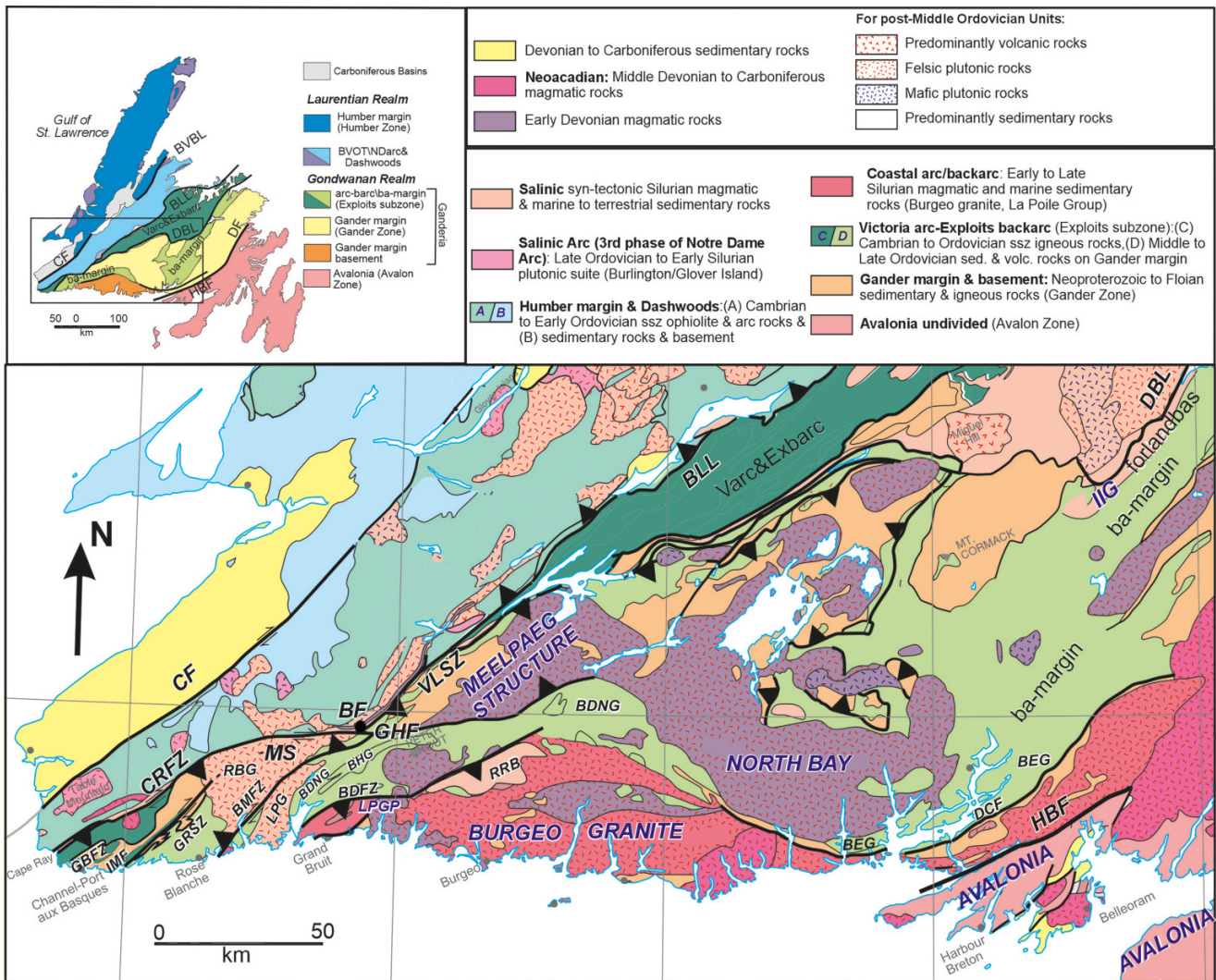

fault zones of the Meelpaeg structure thus had terminated by the Middle Devonian, which was confirmed by the detailed structural and geochronological investigations of the CRFZ by Dubé et al. (1996).

Geochronological evidence suggests the Meelpaeg tectonites between the CRFZ and BMFZ in southwestern Newfoundland were intensely deformed (van Staal et al. 1992; Lin et al. 1993) and metamorphosed to upper amphibolite facies conditions during the latest Silurian to earliest Devonian (Dunning et al. 1990; Burgess et al. 1995; Valverde-Vaquero et al. 2000). Allochthonous tectonites metamorphosed to relatively high pressures (10–8 kb) and temperatures (650–750 °C)

(Burgess et al. 1995) during the Silurian to Early Devonian are relatively rare in Newfoundland and the Canadian Appalachians in general and hence these rocks provide insight into the tectonic processes that were active in the infrastructure of the Salinic and Acadian orogenies and have an important bearing on the formation and tectonic evolution of the Meelpaeg structure. Lin et al. (1994) interpreted formation of these Meelpaeg tectonites in southwestern Newfoundland as due to wedging and west-directed thrusting of a tectonic flap of high-grade rocks during the final stages of the late Silurian to Devonian collision between a promontory on the Gander margin (Cabot promontory) and the St. Lawrence

Fig. 2. (A) Simplified geology of southwestern Newfoundland modified from van Staal et al. (1996*a*, 1996*b*). Ages and metamorphic zones compiled from Dunning et al. (1990), Burgess et al. (1995), Dubé et al. (1996), and Valverde et al. (2000) and those presented herein. The map units are labelled in the right lower corner. The antiform–synform symbols for major F2 and F3 folds are open and solid black, respectively. In addition, the line weight is higher for F3. Some of the units and details shown in cross-sections B and C have been omitted on the map for the sake of clarity but can be seen in the detailed maps of Figs. 5 and 6. Upper Ordovician to Silurian rocks of the Windsor Point Group lie unconformably on the older rocks of the Dashwoods terrane (Dubé et al. 1996). (B) Cross-section (A-A') through the Grand Bay Complex and Port aux Basques Complex. (C) Cross section (B-B') through Harbour le Cou Group and eastern part of Port aux Basques Complex. Down plunge projections are interpretive and schematic due to non-cylindricity of F3 folds and unknown structural complexities at depth. Abbreviations are partly given in Fig. 1. BBF, Big Barachois fault; BIBA, Burnt Island Brook anticline; DRD, Dolphin Road dome; GRSZ, Grandys River shear zone; GSA, Grandy Sound antiform; IMDZ, Isle aux Morts deformation zone; IMF, Isle aux Mort Fault; OBF, Otter Bay Fault.
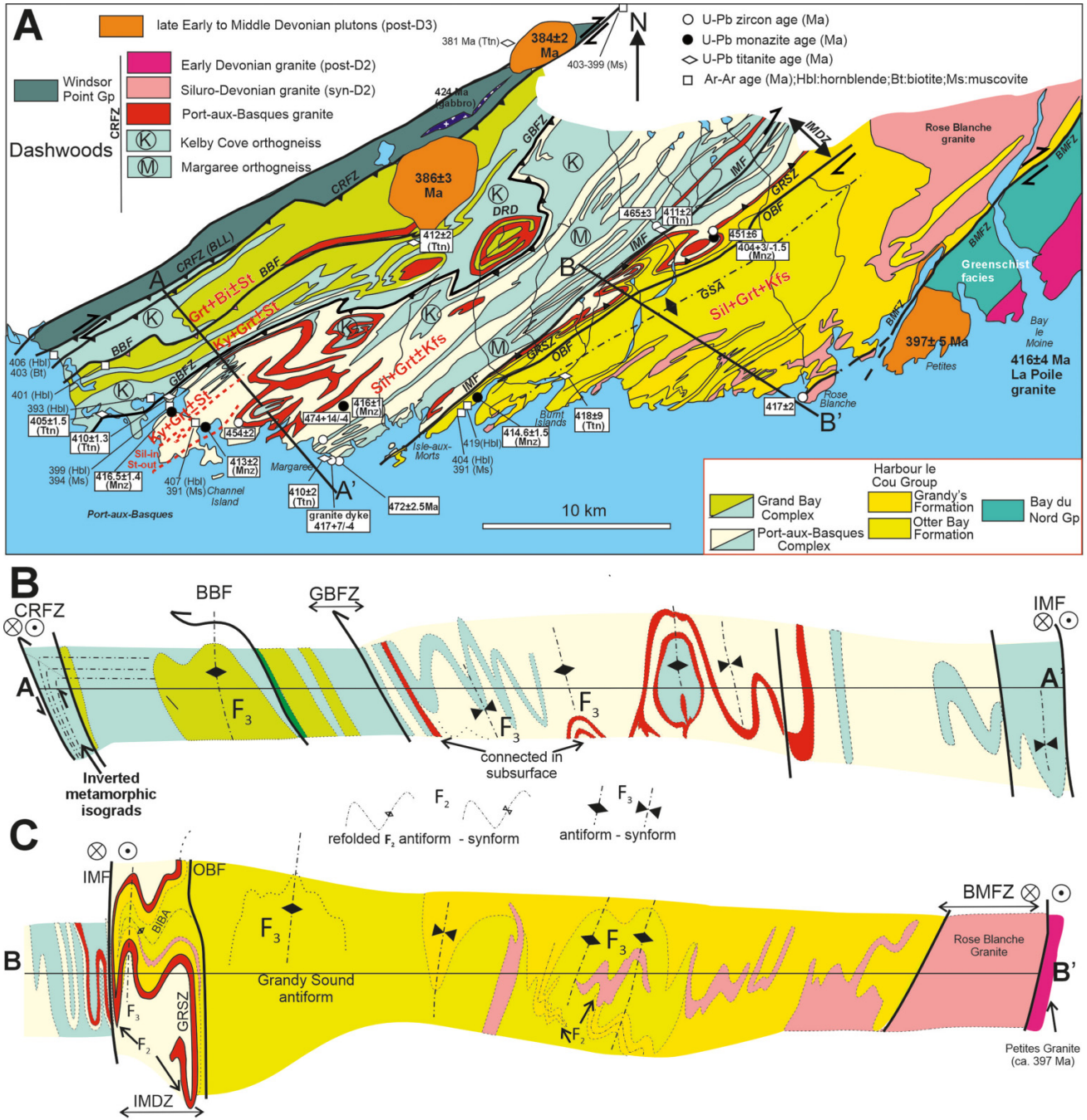
promontory on the Laurentian margin. The deformation discussed herein thus may also provide further insight on the tectonic role of promontories and comparison of the structures formed in the re-entrant further to the northeast (e.g., Lafrance and Williams 1992; Zagorevski et al. 2007; van Staal et al. 2014a; Willner et al. 2018; Honsberger et al. 2022) versus those in the adjacent promontories during collision.

Southwestern Newfoundland is characterized by generally excellent and nearly continuous exposure in a ca. 5–7 km wide strip along the coast. The results of detailed structural analysis combined with geochronological and petrological investigations in this part of Newfoundland are presented herein.

Geological units

The amphibolite facies Meelpaeg tectonites between the CRFZ and BMFZ (Fig. 2) have been divided into three major polyphase-deformed lithological units (van Staal et al. 1996a, 1996b; Schofield et al. 1998) that are separated by fault zones. From west to east, these are the Grand Bay Complex (GBC), Port aux Basques Complex (PABC), and the Harbour Le Cou Group (HLCG). The geology of the central PABC has a bearing on interpretations of the other two units and is therefore described first.

Port aux Basque Complex (PABC)

The PABC is separated from the GBC to the west by the Grand Bay Fault zone (GBFZ). To the east, it is separated by Grandys River shear zone (GRSZ), part of the wider Isle aux Morts deformation zone (IMDZ), from the HLCG (Figs. 1, 2, and 5). The supracrustal rocks of the PABC (Figs. 3A, 3C, 4B, 4E, and 4G) are mainly represented by quartz-rich metasandstone rhythmically interlayered to varying degrees with pelitic and semipelitic layers, which were metamorphosed into paragneiss and garnet, kyanite, or sillimanite-bearing schist, respectively. The metasandstone beds are distinctive and correlate with the Cambrian to Lower Ordovician Gander Group elsewhere in Newfoundland (Ganderia's cover sequence 1 or GCS1; van Staal et al. 2021). Sedimentary structures are rarely preserved, but grading (Fig. 4G) and cross-bedding (van Staal et al. 2021; Fig. 5B) occur in a few places. The rocks are intruded by a regionally extensive swarm of pre-tectonic mafic dikes (Schofield et al. 1998); felsic to mafic intrusive bodies of the Floian to Darriwillian Margaree and Kelby Cove orthogneisses (Fig. 2); and narrow sheets of the Upper Ordovician Port aux Basques granite (Fig. 3H) (Valverde-Vaquero et al. 2000, 2006). The generally narrow Port aux Basques granite sheets, commonly well outlined on air photos, cut all other pre-tectonic igneous and supracrustal rocks and are complexly folded (Figs. 2, 3H, and 5). Hence, the Port aux Basques granite represents an important structural and time marker, especially considering that the Port aux Basques granite is absent in the HLCG, east of the GRSZ (Figs. 2 and 5). Although transposition and rare preservation of sedimentary structures prevented erection of a regionally mappable subdivision of the metasedimentary rocks, the structurally lowest and possibly oldest rocks of the PABC are represented by medium-to-thinly bedded mica-poor, metasandstone (Figs. 3C and 4E). Thin red coticule beds occur in some of the thicker metasandstone beds and are common in Middle Cambrian rocks of the GCS 1 (van Staal et al. 2021), suggesting that the oldest rocks of the PABC are Middle Cambrian and/or older. Structurally above these rocks, rhythmically interlayered dark, graphite-bearing schist layers become more common (Fig. 4G). These sedimentary rocks are correlated with the upper Cambrian to early Floian rhythmically interlayered metasandstone and black shale of the GCS1.

The Margaree orthogneiss comprises a relatively juvenile (Whalen et al. 1997) mafic to felsic intrusive complex. Mingling of the mafic and felsic rocks indicate they are coeval (Valverde-Vaquero et al. 2000). The composition of the igneous rocks varies from arc tholeiite to within-plate basalt in the intrusive mafic amphibolite dikes, suggesting a rifted arc setting that developed into a backarc basin (Schofield et al. 1998). The Margaree orthogneiss yielded U–Pb zircon TIMS ages between 474 and 465 Ma, which combined with the U–Pb zircon dates between 454 Ma (Fig. 2, Valverde-Vaquero et al. 2000, 2006) and 451 Ma (see U–Pb geochronology section below) of the cross-cutting Port aux Basques granite (van Staal et al. 1996a, 1996b) suggest that all the orthogneiss and pre-tectonic amphibolite intrusions in the PABC are late Early-to-Middle Ordovician.

The Upper Ordovician Port aux Basques granite (Fig. 3H) is a distinct suite of narrow white to red biotite and locally hornblende-bearing granitoid sheets, which have compositions ranging from low-K tonalite to granite (Whalen et al. 1997). They represent the last gasp of magmatism associated with the complex Floian to Katian evolution of the Victoria arc and Exploits backarc in this part of Newfoundland (Valverde-Vaquero et al. 2006; Zagorevski et al. 2010).

The PABC is thus a composite terrane comprising intrusive bodies related to the Victoria arc and Exploits backarc evolution, and an older Gander margin substrate (Fig. 1). Members of the older Penobscot arc, which locally underlie the Victoria arc further to the north (Zagorevski et al. 2010), have not been recognized but may be present as suggested by Schofield et al. (1998). A Gander margin substrate to the Victoria arc with few exceptions (Rogers et al. 2006) is largely unexposed elsewhere in Newfoundland but identified on basis of isotopic and inherited zircon data (Zagorevski et al. 2008, 2010). It indicates that part of the Gander margin after Early Ordovician obduction by elements of the Penobscot arc and associated backarc (Colman-Sadd et al. 1992; Zagorevski et al. 2010) became the substrate to the Victoria arc, which in turn was subjected to Middle Ordovician backarc rifting (Valverde-Vaquero et al. 2006). The Gander margin thus was modified during two successive stages of backarc opening and closing (van Staal et al. 2021; van Staal and Barr 2012).

Grand Bay Complex (GBC)

The GBC is the most western unit and is sandwiched between the CRFZ in the west and the GBFZ in the east (Fig. 2). The GBC rocks are generally highly strained tectonites dissected by moderately to steeply southeast-dipping shear zones (Figs. 3D and 3G). Hence stratigraphic relationships could not be deciphered among its supracrustal rocks. This

Fig. 3. A: Subvertical outcrop of PABC straight gneiss tectonite immediately west of the Isle aux Morts fault with backrotated swells in well-foliated Margaree aplite, which indicate shear towards the northwest (left). Quartz-rich veins in the tectonite are isoclinally folded and strongly boudinaged, all consistent with high non-coaxial strains. Fieldbook on horizontal ledge for scale, (B) Subvertical outcrop with steeply plunging mineral/stretching lineation defined by sillimanite nodules and garnet porphyroblasts with sillimanite pressure shadows in S2 in Otter Brook Formation of the HLCG. Monazite of sample 93GD16 (Fig. 7) was collected at this outcrop; (C) Brittle reverse fault with movement to the northwest (left) in PABC tectonites in town of Port aux Basques. Claudia Riveros for scale, (D) small-scale thrust in Kelby Cove orthogneiss tectonite in GBC in the footwall of the GBFZ, (E) Sinistral S-C fabric in intrusive syntectonic Rose Blanche granite sheet caught up in the IMDZ. Note that the sinistral fabric is overprinted by a small dextral shear zone near the bottom of photograph, (F: Southerly or southeasterly overturned, nearly recumbent F2 fold in white Rose Blanche granite aplite that cut strongly foliated (S1 and S2) rusty metasandstone and pelite of the Otter Bay Formation of the HLCG. The fold is less tight than isoclinal F2 folds in the country rock (poorly visible) and the S2 foliation is weakly developed or absent in the granite, consistent with other evidence that intrusion took place during D2. The folds and S2 are openly folded by F3 because the D1-2 structures are situated in the hinge of a large shallowly northeast plunging F3 fold. Note the oblique boudinage of a narrow granite vein with respect to Sm, suggesting the thicker granite aplite was buckled when it moved into the shortening field from an orientation at a high angle to the extension direction indicated by the extended narrow vein, which is assumed to have progressively rotated into the field of extension during D2-related, southeast-directed shear (to the right). Person for scale. (G) Mushroom interference pattern between isoclinal F2 and tight F3 folds in Kelby Cove felsic orthogneiss tectonite in the GBC with strong S1 between the CRFZ and GBFZ. Note the curviplanar nature of the F3 axial surfaces indicating dextral sense of shear. (H) GRSZ tectonite in the Port aux Basques granite with intrafolial F2 fold of S1 refolded by open to close F3 folds. Abbreviations in Figs. 1 and 2. PABC, Port aux Basques Complex; HLCG, Harbour Le Cou Group; GBC, Grand Bay Complex.
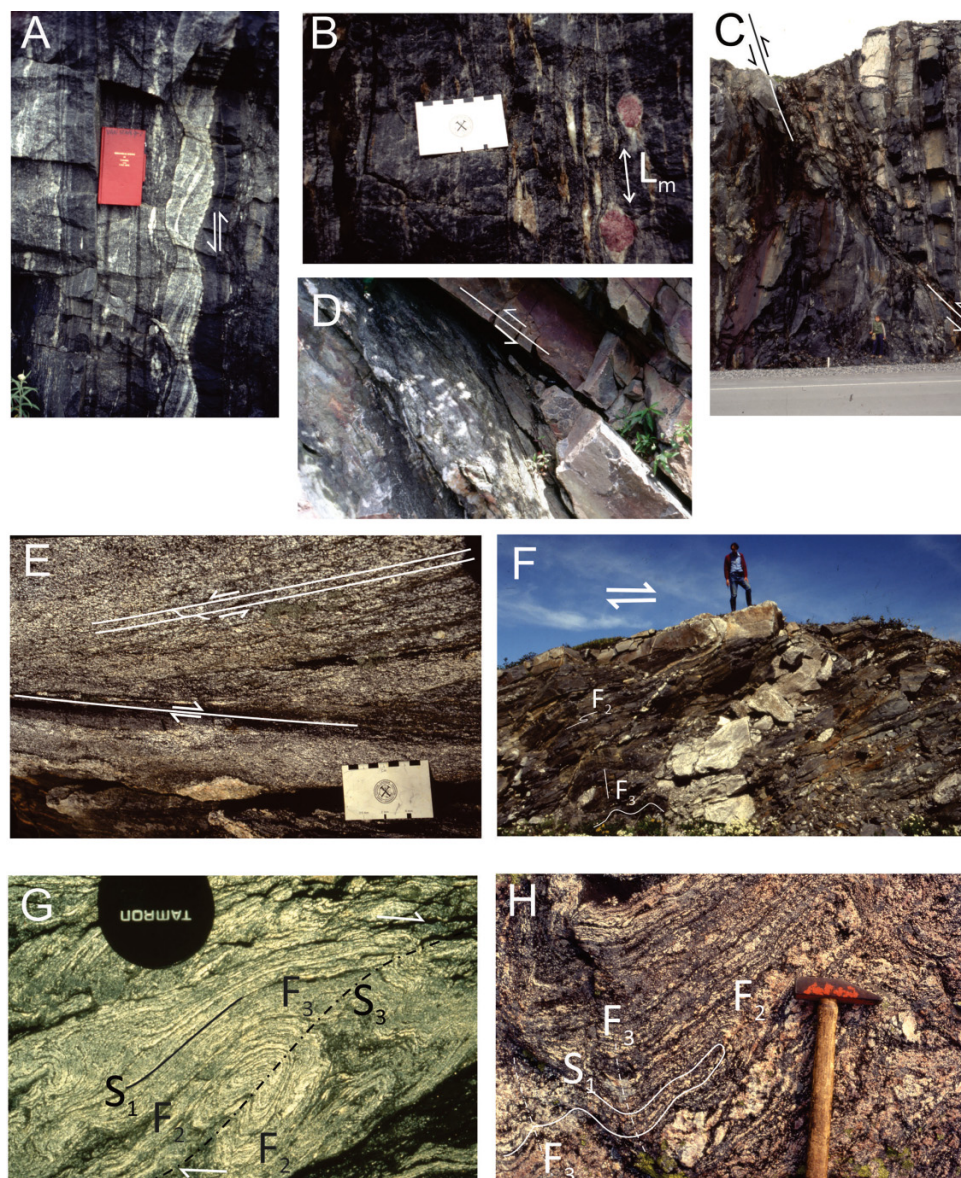
Fig. 4. (A) Refolding of F1 isocline by reclined F2 fold in thin-bedded rusty psammite and pelite of the Grandy's Formation of the HLCG; S2 is moderately dipping towards the north. Small-scale F3 folds are not visible; (B) Refolding of F2 isocline in metasandstone and semi-pelite of the PABC by open to close F3. Well-developed S1 folded by F2 includes strongly attenuated Port aux Basques granite veins; (C) Recumbent F2 sheath and curtain folds in Otter Bay Formation metasandstone of the HLCG with lineation parallel to F2 and small open F3 with weak S3; (D) Doubly plunging, tight disharmonic F3 buckle folds in red coticule layers in sillimanite schists of the Grandy's Formation of the Harbour Le Cou Group. This type of plunge reversal produced the map-scale F3 domes; (E) Fishhook like interference pattern between F3 and F2 folds in PABC metasandstone and narrow pegmatite vein mimicking the large-scale interference pattern shown by the Port aux Basques granite that defines the GRSZ; (F) Stretching lineation (Ls) in HLCG folded by F3 fold; (G) upright upwards facing F3 fold (for space reasons rotated 90° to right in photo) in graded metasandstone-pelite of the PABC. Grading is best recognized by the progressive refraction of S3; (H) Strongly curvilinear F3 fold in PABC folding an older mineral/stretching lineation. A younger mineral lineation is parallel to the F3 hinge line. PABC, Port aux Basques Complex; HLCG, Harbour Le Cou Group; GRSZ, Grandys River shear zone.
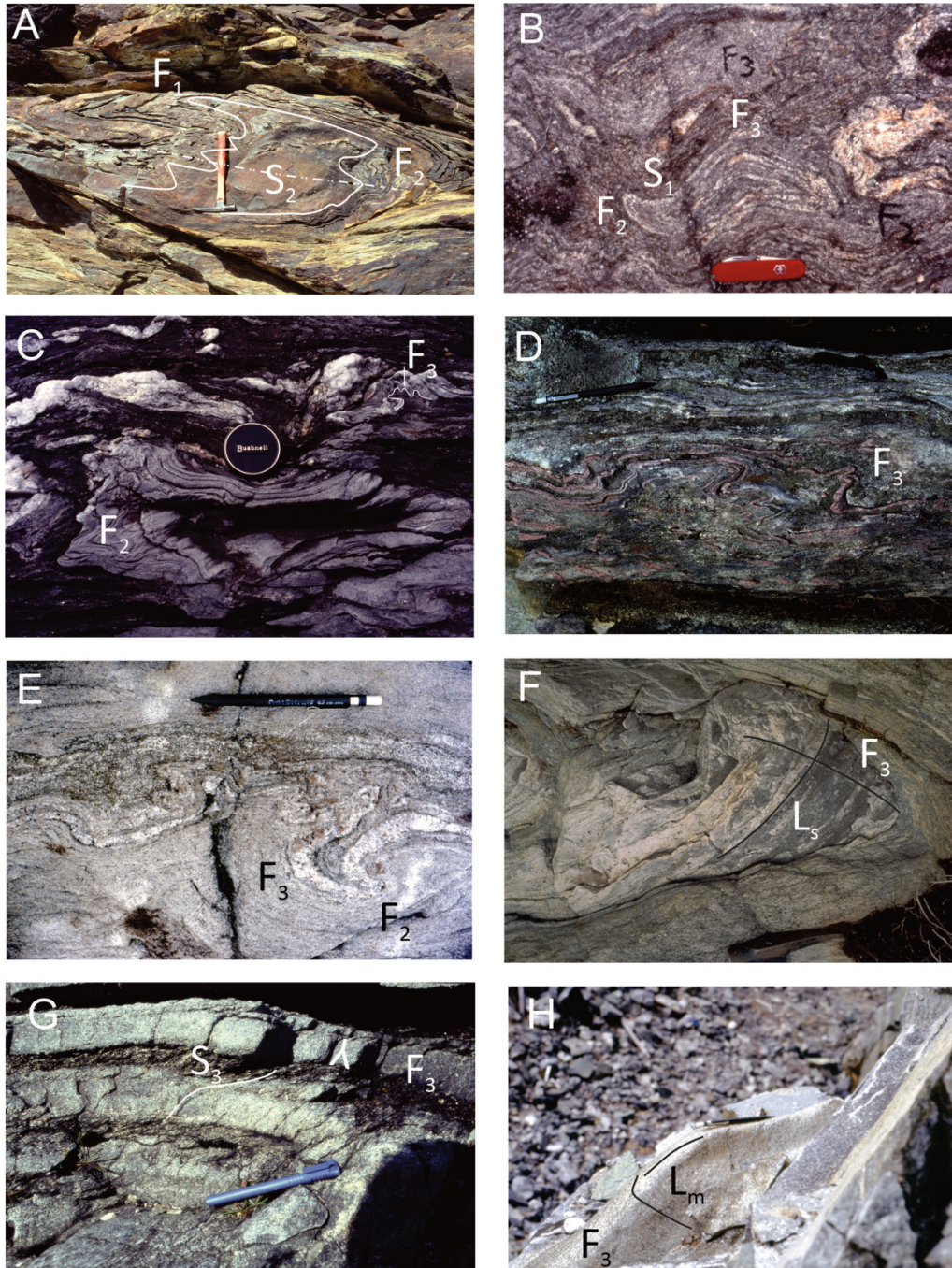
Fig. 5. (A) Geology of the Isle aux Morts deformation Zone (IMDZ) with lower hemisphere equal area projections of the main structural elements (poles to planes and lineations); F3n and F3s refer to small-scale F3 folds on the north limb and south limbs of the F2 Burnt Island Brook structure, respectively. The old (pre-F2) Grandys River shear zone (GRSZ) is outlined by solid black line with barbs on the hangingwall, whereas D3 transcurrent faults are marked by relatively heavy dashes and dots. Contacts of lithological units are finely dashed and where inferred are dotted. The F2 folds are characterized by two ticks along the trace of their axial surfaces, whereas three ticks outline F3 axial surfaces. The symbols for antiform and synform of F2 and F3 are open and solid, respectively (also see Fig. 2). BIF, Burnt Island Faults; IMF, Isle aux Mort fault (proper); OBF, Otter Bay fault; P, pillow basalt. (B) Three-dimensional sketch of the interference pattern of the Port aux Basques granite (red) that defines the GRSZ. (C) Photo with cataclasite of the IMF in small tributary of the Grandys River. A young Pablo Valverde-Vaquero for scale. GRSZ, Grandys River shear zone
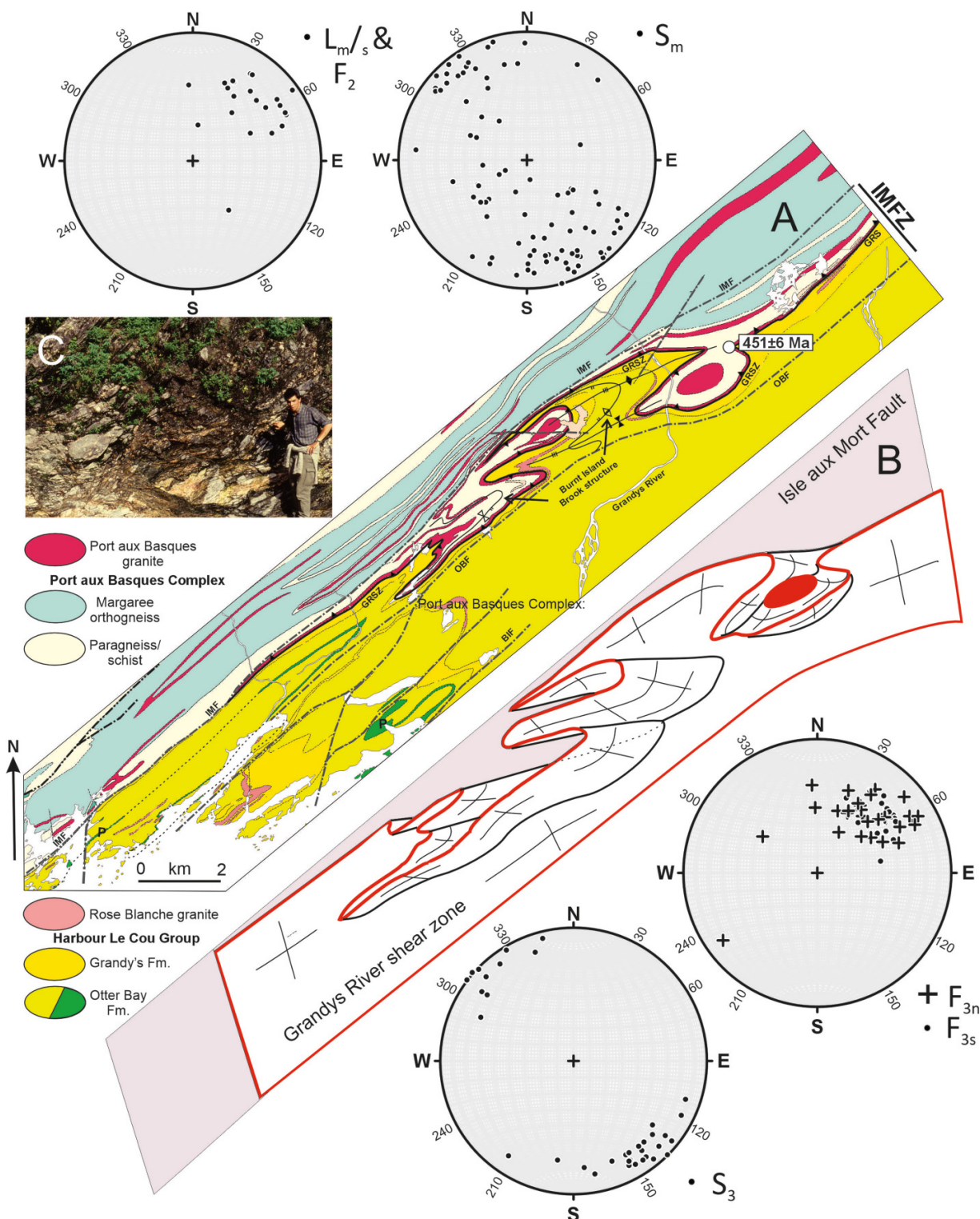
unit mainly comprises rhythmically alternating garnet, staurolite, and kyanite-bearing micaceous schist, which are locally migmatized, coticule beds, orthogneiss and mafic amphibolite sheets of various thicknesses (van Staal et al. 1996a; Burgess et al. 1995; Schofield et al. 1998).

Intrusive relationships are locally preserved between the metasedimentary rocks of the GBC, the felsic to mafic members of the pre-tectonic Kelby Cove orthogneiss (Figs. 3D and 3G) and the transposed amphibolite dikes like those in the PABC. The felsic gneisses comprise hornblende and/or biotite-bearing tonalite to granite, whereas amphibolite and rare cummingtonite-bearing hornblendite represent metamorphic mafic and ultramafic (pyroxenite) rocks (van Staal et al. 1996a, 1996b). The Kelby Cove orthogneiss has geochemical compositions very similar to the Floian to Darriwilian (474–465 Ma) Margaree orthogneiss of the adjacent PABC (Valverde-Vaquero et al. 2000), which is therefore interpreted to be consanguineous (Schofield et al. 1998). This is supported by the preserved intrusive relationships between the Late Ordovician Port aux Basques granite (Figs. 3H and 4E) and the older Kelby Cove orthogneiss and amphibolite dikes.

The metasedimentary rocks of the GBC are interpreted to have been deposited above the PABC based on two lines of evidence: (1) metasandstone and metapelite characteristic of the PABC, inferred to be early Floian or older in age, occur structurally below metasedimentary rocks of the GBC in the cores of large antiforms such as the Dolphin Road dome (Fig. 2, DRD), and (2) a close stratigraphic relationship must have existed between the GBC and the PABC before intrusion of the Middle-to-Late Ordovician stitching mafic and felsic intrusions and subsequent tectonism (see below). The metasedimentary rocks of the GBC are therefore inferred to have been deposited during the Floian to Dapingian, which is consistent with the common presence of coticule layers. A horizon of coticules (Fig. 4D) occurs in Dapingian sedimentary rocks of the Gander cover sequence 2, which was disconformably deposited on the Gander margin after the Penobscot orogeny (van Staal et al. 2021).

Harbour Le Cou Group (HLCG)

The Harbour Le Cou Group (HLCG) occurs east of the GRSZ (Figs. 2 and 5) and is separated from Ordovician greenschist facies rocks of the Bay du Nord Group (Blackwood 1984; Dunning et al. 1990; Tucker et al. 1994) by the BMFZ (Figs. 1, 2, and 6) (Lin et al. 1993; van Staal et al. 1996b). The HLCG forms part of an extensive belt of Floian to Late Ordovician metasedimentary rock (Fig. 1 inset), which includes the Baie d'Espoir, Red Cross, and Bay du Nord groups (eastern half of Exploits subzone of Williams et al. 1988, 1993) that were disconformably deposited on the Gander Group and correlatives (Colman Sadd et al. 1992; Valverde-Vaquero et al. 2006). These rocks were referred to as the Gander cover sequence 2 (GCS 2) by van Staal et al. (2021) and have been interpreted to form part of the Gander margin of the Exploits backarc basin (van Staal 1994; Valverde-Vaquero et al. 2006).

The distinctive metasedimentary rocks of the HLCG have been subdivided into two formations (Fig. 2). Sedimentary structures such as grading suggest that the Otter Bay For-

mation (Figs. 3B and 3F) is older than the structurally overlying Grandy's Formation (Fig. 4A) (van Staal et al. 1996b). The Otter Bay Formation consists of thick- to thin-bedded feldspathic metasandstone rhythmically alternating with thin beds of rusty, pyritiferous semi-pelite metamorphosed to sillimanite–garnet schist (Fig. 3F). The metasandstone layers commonly contain garnet, clinopyroxene, clinozoisite, and hornblende-bearing calc-silicate pods or lenses; similar rocks occur in the Baie d'Espoir Group (Salmon River Dam Formation of Colman-Sadd (1980)). Minor bodies of massive sulfide and associated pillowed tholeiitic metabasalt are also present in the Otter Bay Formation (Figs. 2 and 5) (van Staal et al. 1992; Lin et al. 1993; Schofield et al. 1998). The pillowed metabasalt occur near the contact with the overlying Grandy's Formation, which mainly consists of rusty garnet–sillimanite schist, thin-bedded metasandstone, coticule (Fig. 4D), and rare metaconglomerate bands (van Staal et al. 1996b, 2021). Coticules in the Grandy's Formation occur near its basal contact with the Otter Bay Formation and are typical for the lithologically similar Dapingian units in the GCS2 (van Staal et al. 2021), such as the Isle Galet Formation of the Baie d'Espoir Group (Colman-Sadd 1980; Blackwood 1985), the ages of which were constrained by fossils and/or by U–Pb zircon ages (Colman-Sadd et al. 1992).

The HLCG was subjected to a similar structural and metamorphic history as the adjacent PABC and GBC (van Staal et al. 1992; Lin et al. 1993; Burgess et al. 1995). However, the extensive intrusive igneous rocks, such as the Margaree orthogneiss and the Port aux Basques granite, which occur west of the GRSZ (Figs. 1 and 2) are absent, indicating the HLCG and PABC were geographically separated during the Middle-to-Late Ordovician. Instead, the HLCG contains bodies of the Rose Blanche granite pluton (Fig. 3F), comprising a distinctive white-to-pink two mica ± garnet granite. The Rose Blanche granite cuts all units of the Meelpaeg structure (Fig. 1)) and provides a minimum age when all units were tectonically assembled.

Bay du Nord Group

The Bay du Nord Group occurs east of the BMFZ (Fig. 6) (Lin et al. 1993; van Staal et al. 1996b) and is lithologically similar to the HLCG, mainly comprising greenschist facies (biotite zone) metasandstone and metapelitic rocks with minor felsic metatuffaceous rocks (O'Brien 1987, 1988). The deformation history is similar to that observed in the adjacent HLCG (Lin et al. 1993). The Bay du Nord Group is intruded by the 416 ± 4 Ma feldspar megacrystic La Poile granite (Chorlton and Dallmeyer 1986), offshoots of which locally have intruded the Rose Blanche granite on the west side of the BMFZ, which separates the two granite bodies (Fig. 1). The Bay du Nord Group continues to the east (Chorlton 1980; Blackwood 1984) and grades further to the east along strike (Colman-Sadd et al. 1990) into the Middle to Upper Ordovician Baie d'Espoir Group (Fig. 1) (Colman-Sadd 1980; Blackwood 1983), supported by a ca. 466 Ma U–Pb zircon age for a felsic tuff in the Bay du Nord Group (Dunning et al. 1990). The Bay du Nord Group comprises at least three fault-bounded belts (Tucker et al. 1994). Rocks of the North Bay belt, which

Fig. 6. (A) geology of the Bay Le Moine fault zone (BMFZ) modified from van Staal et al. (1996b). The steeply northwest-dipping fault zone had a prolonged history of movement that started during at least D2, since D2 mylonites were cut by later phases of the same granite and overprinted during D3. High strain accumulated on both sides of the fault zone but became progressively localized over time culminating in a dextral brittle fault that offsets the late Early Devonian Petites Granite. (B) Mylonite in white Rose Blanche granite in BMFZ with dextral shearbands in boudinaged syntectonic, less strained cross-cutting aplite of same granite attesting to syn-D2 movements. Thin white aplite veins are isoclinally folded (F2) within Sm.
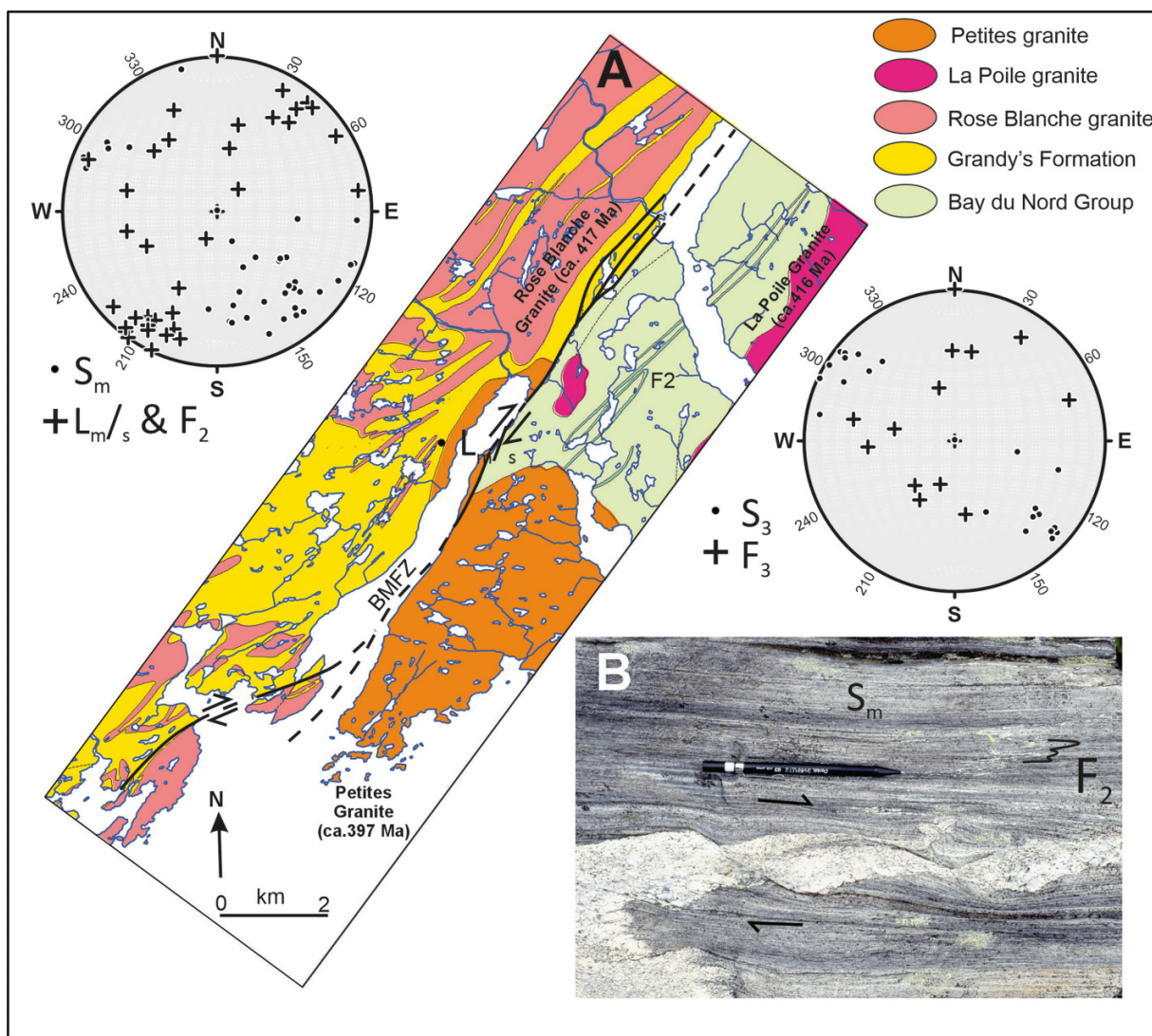
are host to massive sulfide deposits and lie adjacent to the southern part of the HLCG, are most pertinent to this study. The North Bay Belt was interpreted to be Middle Ordovician based on regional correlations (Colman-Sadd et al. 1990) and the age of the dated felsic tuff but parts were inferred to be intruded by offshoots of the Baggs Hill granite (Fig. 1, BHG), which yielded a U–Pb zircon TIMS date of ca. 478 Ma (Tucker et al. 1994). The inferred intrusive relationship was based on an undated granite dike correlated with the dated Baggs Hill pluton. However, we observed a conglomerate containing clasts of the Baggs Hill granite along the sheared contact between the North Bay belt and the Baggs Hill granite on the north side of Rocky Ridge near the dated locality of Tucker et al. (1994), suggesting that at least this part of the North Bay belt lies unconformably above the granite. Hence, either

the North Bay belt is Middle Ordovician and not Lower Ordovician, or the North Bay belt is a composite unit locally including rocks that are older than 478 Ma.

U–Pb geochronology

Analytical technique

Sample preparation and U–Pb ID-TIMS analytical methods and instrumentation are similar as those described in Valverde-Vaquero et al. (2006). The Port aux Basques granite (Vl-02-17) was dated at the Geological Survey of Canada in Ottawa, whereas the monazites and titanites of six metamorphic tectonites and zircon of the Rose Blanche granite were dated at Memorial University of Newfoundland. Con-

cordia ages and U–Pb Concordia diagrams were drawn and calculated with Isoplot (Ludwig 1999).

Port aux Basques granite in Grandys River shear zone

A Port aux Basques granite tectonite from the GRSZ (VL-02-17; Z7825) was sampled (Fig. 2) to: (1) test whether the distinctive Port aux Basques granite, which was previously dated further to the west outside the IMDZ near the type locality (454 ± 2 Ma, Valverde-Vaquero et al. 2006), had a consistent age separate from the other gneissic granitoid bodies in the PABC and (2) to constrain the age of structural juxtaposition of the PABC and HLCG. Three multigrain zircon and four monazite single crystal fractions were analysed from this sample. The zircon fractions, ranging from 32 to 61 crystals (number of individual crystals of each fraction given in brackets), were pre-treated with the mechanical, air-abrasion method of Krogh (1982) to remove areas affected by secondary Pb loss. The three fractions are 1.2%–1.5% discordant, overlap the Concordia between 444 and 447 Ma, and yield a Concordia age of 446 ± 1.5 Ma with an mean square weighted deviation (MSWD) of 3.5 and a low probability of concordance (Fig. 7). This suggests that these fractions are affected by some degree of secondary Pb loss. Hence the Concordia age probably represents a minimum age. The $^{207}Pb/^{206}Pb$ ages of these three fractions are almost identical and yield a weighted average age of 451.4 ± 3.5 Ma (MSWD 0.16). The upper intercept age of a discordia line anchored at 0 ± 50 Ma calculated with the Monte Carlo solution yields an age of 451.3 $^{+5.6}/_{-5.7}$ Ma. Since the upper intercept age overlaps the Concordia and weighted $^{207}Pb/^{206}Pb$ average age, an age of 451 ± 6 Ma is considered as the best estimate of zircon crystallization age of the Port aux Basques granite. This age overlaps within error with the age of 454 ± 2 Ma reported by Valverde-Vaquero et al. (2006) for this granite near its type locality.

The four single crystal monazite fractions (M1 to M4; Table 1), which were not abraded, plot around 404–410 Ma on the Concordia curve (Fig. 7A). Monazite M4 has a large error due to the abundance of common Pb and will not be discussed. Monazite M2 is concordant at 404 Ma, while monazites M1 and M3 have a slight reverse discordancy (−1.1%) and touching Concordia at ca. 407 Ma. All these three analyses are very clean, less than 3 pg common Pb, and they all have matching $^{207}Pb/^{206}Pb$ ages with an average weight age of 403.8 ± 1.4 Ma (MSWD 0.26). This suggests that the reverse discordancy could be due to U loss. Therefore, expanding the errors to cover the maximum possible age, an age of 404 $^{+3.5}/_{-1.5}$ Ma is the best estimate for the age of monazite formation.

The monazite crystallization age overlaps with part of the Ar–Ar hornblende and biotite ages (407 to 401 Ma) measured in the PABC and HLCG (Figs. 2 and 8); however, it is ca. 10 my younger than monazite and most of the titanite ages compiled in Fig. 2 (Dunning et al. 1990; Burgess et al. 1995; Dubé et al. 1996; Valverde-Vaquero et al. 2000; this study). The age of 404 Ma is therefore best interpreted as a new phase of monazite growth, during localized D_3 deformation localized in the IMDZ, while regional cooling of the surround-ing GBC, PABC, and HCLG had reached the blocking temperature of hornblende (ca. 500 °C) and locally also biotite (Fig. 2).

Rose Blanche granite

The Rose Blanche granite (sample 92GD12) yielded eu-hedral zircon needles, which were analyzed as two zircon multigrain fractions. Fraction Z1 is concordant and yields a $^{207}Pb/^{206}Pb$ age of 419 ± 5 Ma and Concordia age of 417 ± 2 Ma (MSWD 0.3) (Fig. 7). A Discordia line anchored on fraction Z1 yields a 417.6 $^{+3.2}/_{-2.5}$ Ma upper intercept age. The Concordia age of 417 ± 2 Ma is judged as the best estimate for zircon crystallization, which is considered a preliminary age due to analysis of only two multigrain fractions.
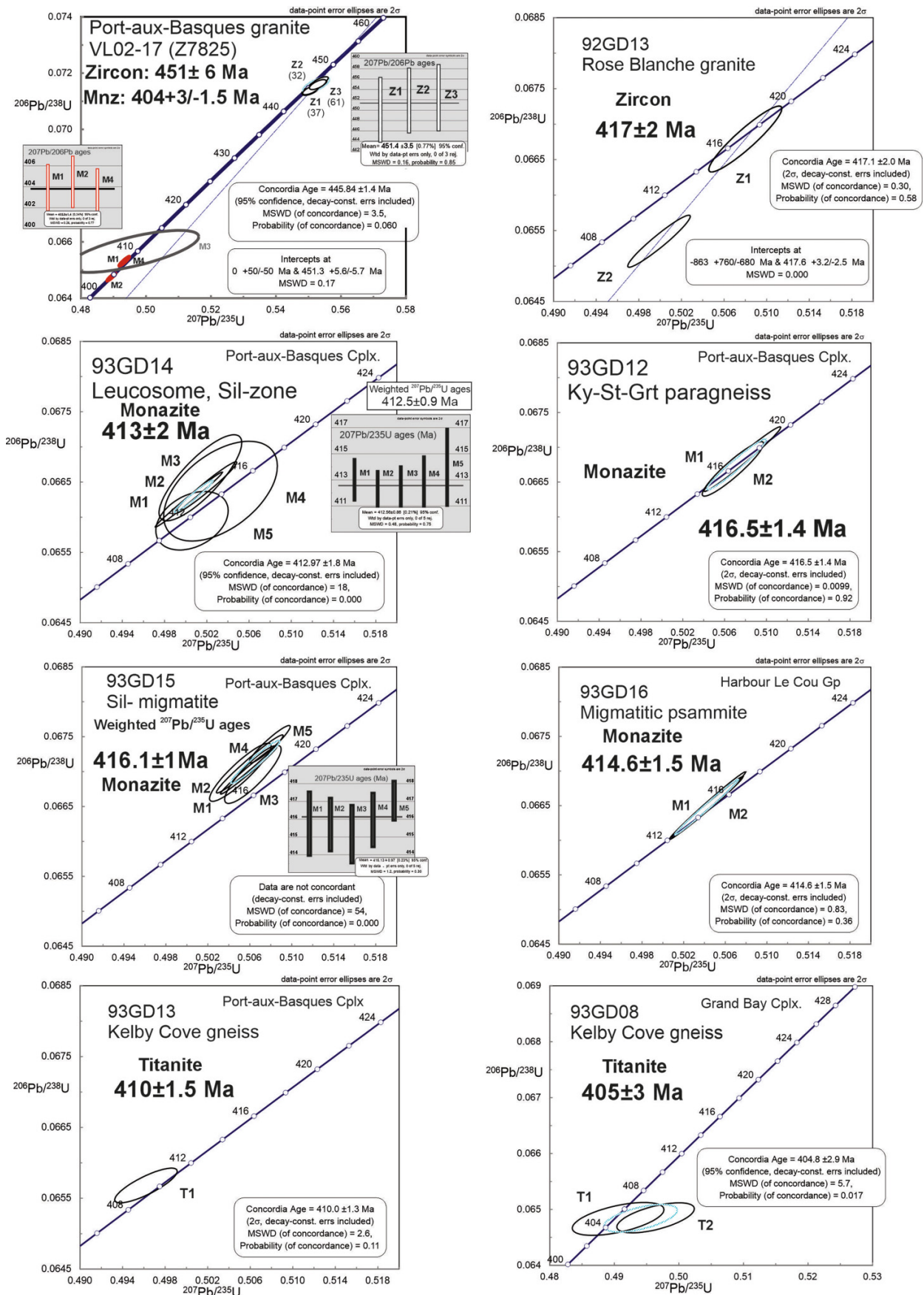
Monazite in metamorphic tectonites of the PABC and HLCG

U–Pb dating of monazite (Fig. 7B) was done in parag-neisses and schists of the PABC and the nearby HLCG to better constrain the timing of the structural and metamor-phic processes during the final stages of D_2 and the onset of D_3 deformations. Sample 93GD12 is a Ky–St–Grt-bearing schist of the PABC sampled near the boundary (GBFZ) between the GBC and PABC (Fig. 2). Two concordant multigrain monazite fractions (M1 and M2) yield a Concordia age of 416.5 ± 1.4 Ma (MSWD, 0.01). Sample 93GD14 is a migmatitic leucosome from sillimanite-bearing schists collected near the ferry docks at Port-aux-Basques (Fig. 2). Three multigrain and two single-grain monazite fractions form a cluster of con-cordant/subconcordant analysis, some reversely discordant, which yield a Concordia age of 413 ± 2 Ma (MSWD 18). The reverse discordance may be due to excess ^{206}Pb. Therefore, the weighted average of the $^{207}Pb/^{235}U$ ages (412.6 ± 0.9 Ma; MSWD 0.48) could be considered more reliable. However, we consider that a larger error age of 413 ± 2 Ma is a more realis-tic estimate of monazite crystallization age. Sample 93GD15 is migmatitic sillimanite and K-feldspar-bearing schist near the village of Margaree (Fig. 2). Three multigrain and two sin-gle grain fractions yield a reversely discordant cluster sug-gesting excess ^{206}Pb. This cluster yields a weighted average $^{207}Pb/^{235}U$ age of 416.1 ± 1 Ma (MSWD 1.2) providing an estimate for monazite crystallization. Sample 93GD12 is a migmatitic garnet, sillimanite, and K-feldspar bearing parag-neiss (Fig. 3B) of the Otter Bay Formation northeast of Isle aux Morts near the Otter Bay fault (Fig. 2). Two concordant multi-grain monazite fractions yield a Concordia age of 414.6 ± 1.5 Ma (MSWD 0.83).

Kelby Cove orthogneiss titanite

Two samples of banded Kelby Cove orthogneiss immedi-ately adjacent to or in the GBFZ (Fig. 2) were analyzed for titanite. Sample 92GD08 is a gneiss from the GBC, and the two multigrain titanite fractions yield a "Concordia age" of 405 ± 3 Ma (MSWD 5.7). Sample 93GD13 is a banded Kelby Cove gneiss from the PABC in the GBFZ; a subconcordant analysis of a titanite fraction provides a Concordia age of 410 ± 1.5 Ma (MSWD 2.6). These ages are within error of the $^{206}Pb/^{238}U$ ages for these fractions, which are least affected

Fig. 7. Concordia diagrams of zircon, monazite, and titanite in rocks of the GBC, PABC, and HLCG and the Port aux Basque and Rose Blanche granites. See text for more details. PABC, Port aux Basques Complex; HLCG, Harbour Le Cou Group; GBC, Grand Bay Complex.

Table 1. ID–TIMS zircon U–Pb geochronological data.

Fraction*	No. Grains	Size (μm)	Description	Wt. ug	U ppm	Pb† ppm	Pb§ pg	206Pb‡ / 204Pb	208Pb / 206Pb	207Pb / 235U	±2SE Abs	206Pb / 238U	±2SE Abs	Corr.¶ Coeff.	207Pb / 206Pb	±2SE Abs	206Pb / 238U	±2SE	207Pb / 235U	±2SE	207Pb / 206Pb	±2SE
Sample: VL-02-17 Port-aux-Basques Granite (Z7825)—GSC laboratory																						
A1 (Z)	37f	80	Co, Clr, Eu, Fz, Nc, St, fln, Pr, DIA	11	220	16	6.6	1654	0.14	0.5508	0.0021	0.07141	0.00014	0.70	0.05594	0.00016	444.6	1.7	445.5	2.7	450.0	6.2
A2 (Z)	32	90	Co, Clr, Eu, Fz, Nc, St, nln, Pr, DIA	17	183	14	11.2	1227	0.15	0.5535	0.0021	0.07171	0.00013	0.73	0.05598	0.00016	446.5	1.6	447.3	2.7	451.6	6.0
A3 (Z)	61	50–100	Co, Clr, Eu, Fz, Nc, St, nln, Pr, Fr, DIA	13	196	14	7.4	1494	0.14	0.5529	0.0021	0.07160	0.00014	0.68	0.05600	0.00016	445.8	1.7	446.9	2.8	452.5	6.3
M1 (M)	1	200	Yellow, Clr, Eu, fln, Mag	1	8078	4955	3.2	10414	9.78	0.4936	0.0012	0.06534	0.00013	0.90	0.05479	0.00006	408.0	1.5	407.3	1.6	403.6	2.4
M2 (M)	1	250	Pale yellow, Clr, An, nln, Fr, Mag	1	9118	4462	2.4	15688	7.67	0.4894	0.0011	0.06475	0.00012	0.91	0.05481	0.00006	404.5	1.4	404.5	1.6	404.6	2.2
M3 (M)	1	175	Yellow, Clr, Eu, fln, Mag	1	8333	5183	320.1	f124.2	9.88	0.4962	0.0164	0.06566	0.00061	0.70	0.05481	0.0015	410.0	7.4	409.1	22.2	404.4	60.1
M4 (M)	1	190	Yellow, Clr, Sub, fln, Fr, Mag	1	8591	6158	5.3	6574	11.61	0.4931	0.0012	0.06529	0.00012	0.89	0.05478	0.00006	407.7	1.5	407.0	1.6	403.3	2.6
Sample: 93GD12 Ky-St-Grt gneiss, Port-aux-Basques Complex—MUN laboratory																						
M1 (M)	Multi	100–180	clr. euh. Abr	179	1912	331	51	28245	1.94	0.507	0.0024	0.06669	0.00032	0.93	0.05511	0.00010	416.2	1.9	416.3	1.6	416.7	4.1
M2 (M)	Multi	100–180	euh. Abr	64	5319	946	70	20491	2.02	0.508	0.0030	0.06683	0.00038	0.98	0.05510	0.00006	417.0	2.3	416.9	2.0	416.3	2.4
Sample 93GD14 Leucosome–Ferry Dock, Port-aux-Basques Complex—MUN laboratory																						
M1 (M)	Multi	100–180	clr euh abr	113	3829	846	764	f	2.79	0.502	0.0024	0.06642	0.00030	f	0.05481	0.00006	414.6	1.8	413.0	1.6	404.5	2.5
M2 (M)	Multi	100	clr euh abr	55	3609	753	50	16583	2.59	0.5	0.0026	0.06625	0.00032	0.99	0.05478	0.00004	413.5	1.9	411.9	1.8	403.3	1.6
M3 (M)	2	>180	lrg. Clr. Abr	10	376	83	14	1111	2.79	0.501	0.0028	0.06595	0.00034	0.34	0.05505	0.00034	411.7	2.1	412.1	1.9	414.3	13.8
M4 (M)	1	>180	lrg. Clr. Abr	5	1925	410	12	3369	2.64	0.501	0.0032	0.06656	0.00050	0.81	0.05463	0.00024	415.4	3.0	412.6	2.2	397.1	9.8
M5(M)	1	>180	lrg. Clr. Abr	5	302	66	14	466	2.80	0.503	0.0044	0.06637	0.00058	0.50	0.05500	0.00048	414.2	3.5	413.9	3.0	412.2	19.5
Sample 93GD15 Sil-migmatite- Margaree Quarry, Port-aux-Basques Complex—MUN laboratory																			f			
M1 (M)	Multi	100–180	clr yel abr	87	4049	1089	88	16828	3.57	0.506	0.0026	0.06711	0.00034	0.98	0.05469	0.00006	418.7	2.1	415.8	1.8	399.6	2.5
M2 (M)	Multi	100–180	clr yel abr	91	4236	1093	106	15399	3.39	0.506	0.0022	0.06702	0.00028	0.99	0.05475	0.00004	418.2	1.7	415.7	1.5	402.0	1.6
M3 (M)	1	>180	clr yel abr	5	7030	1783	8	17683	3.32	0.505	0.0024	0.06699	0.00034	0.90	0.05468	0.00012	418.0	2.1	415.1	1.6	399.2	4.9
M4 (M)	1	>180	clr yel abr	5	4144	1132	6	13480	3.66	0.506	0.0022	0.06696	0.00034	0.86	0.05484	0.00014	417.8	2.1	416.0	1.5	405.7	5.7
M5(M)	2	>180	clr yel abr	10	5292	1316	12	18236	3.21	0.508	0.0016	0.06739	0.00022	0.94	0.05466	0.00006	420.4	1.3	417.0	1.1	398.3	2.5
Sample 93GD16 Migmatitic Psammite—Otter Bay Formation, Harbour Le Cou Group—MUN laboratory																						
M1 (M)	Multi	100–180	clr euh yel abr	109	5434	760	107	23137	1.38	0.504	0.0030	0.06650	0.00040	0.99	0.05499	0.00004	415.0	2.4	414.6	2.0	411.8	1.6
M2 (M)	Multi	100–180	clr pale yel abr	63	5603	822	91	16217	1.50	0.504	0.0028	0.06648	0.00036	0.99	0.05502	0.00004	414.9	2.2	414.6	1.9	413.0	1.6

Canadian Science Publishing

Table 1. (*concluded*).

Fraction[*]	No. Grains	Size (μm)	Description	Wt. ug	U ppm	Pb[†] ppm	Pb[§] pg	206Pb[‡] 204 Pb	208Pb 206Pb	207Pb 235U	±2SE Abs	206Pb 238U	±2SE Abs	Corr.[¶] Coeff.	207Pb 206Pb	±2SE Abs	206Pb 238U	±2SE	207Pb 235U	±2SE	207Pb 206Pb	±2SE
Fract.1																						
Z1(Z)	Multi	120	euh needles abr	16	766	54	7.1	6154	0.18	0.5080	0.0028	0.06679	0.00038	0.93	0.05516	0.00012	416.8	2.3	417.1	1.9	418.7	4.9
Z2(Z)	Multi	120	euh needles abr	58	1636	108	40	8523	0.12	0.4999	0.0024	0.06535	0.00030	0.95	0.05548	0.00008	408.1	1.8	411.6	1.6	431.6	3.2
92GD08 Kelby Cove gneiss, titanite, Grand Bay Complex—MUN laboratory							f															
T1 (Ttn)	Multi	100–180	brown angular abr	307	95	6	1130	329	0.06	0.4906	0.0058	0.06483	0.00024	0.56	0.05488	0.00056	404.9	1.5	405.3	3.9	407.3	22.8
T2 (Ttn)	Multi	100–180	brown raspberry abr	156	183	f	1004	339	0.06	0.4964	0.0049	0.06485	0.00022	0.60	0.05551	0.00046	405.1	1.3	409.3	3.3	432.8	18.5
93GD13 Kelby Cove gneiss, Port-aux-Basques Complex—MUN laboratory							f															
T1 (Ttn)	Multi	120–180	brown abr	176	269	17	584	514	0.04	0.4962	0.0024	f	0.00020	0.82	0.05480	0.00016	410.1	1.2	409.1	1.6	404.1	6.5

[*]Z, zircon fraction (all zircon fractions were mechanically abraded for 2.96 h); M, monazite fraction (unabraded).

Grain descriptions: Co, colourless; Clr, clear; fIn, few inclusions; nIn, numerous inclusions; Fr, fractures; Eu, Euhedral; Sub, subhedral; An, anhedral; Pr, prismatic; Frag, fragment; St, stubby prism; El, Elongate; Fz, faint zoning; Nc, no cores; DIA, diamagnetic fraction; Mag, Mag @0.5 A 10° SS h, respectively.

[†]Radiogenic Pb

[‡]Measured ratio, corrected for spike and fractionation.

[§]Total common Pb in analysis corrected for fractionation and spike.

[‖]Corrected for blank Pb and U and common Pb, errors quoted are 1 sigma absolute; procedural blank values for this study were from 0.1 pg U and 5 pg Pb (for zircon analyses) and 0.1 pg U and 3 pg Pb (for monazite analyses). Pb blank isotopic composition is based on the analysis of procedural blanks; corrections for common Pb were made using Stacey–Kramers compositions.

[¶]Correlation coefficient.

[#]Corrected for blank and common Pb, errors quoted are 2 sigma in Ma. The error on the calibration of the GSC ^{205}Pb–^{233}U–^{235}U spike utilized in this study is 0.22%

Fig. 8. Compilation of all existing ages and their errors used in this paper with respect to the tectonostratigraphy of southwestern Newfoundland looking south. Time scale is from Cohen et al. (2022). In addition to the new age data presented in Fig. 7 and Table 1, it also includes ages from Chorlton and Dallmeyer (1986), Dunning et al. (1990), Burgess et al. (1995), Dubé et al. (1996), and Valverde-Vaquero et al. (2000). Abbreviations are explained in Figs. 1 and 2.
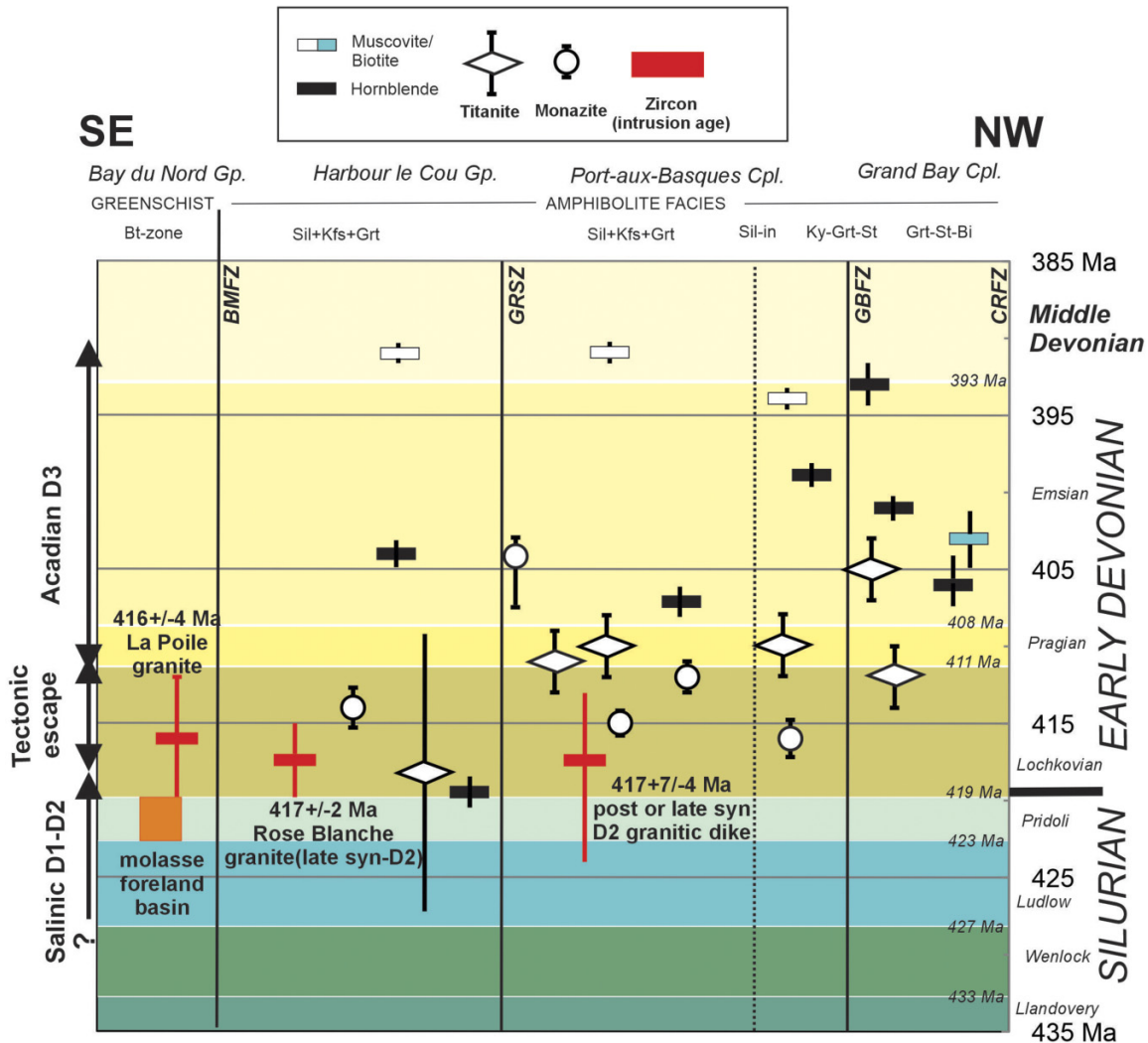
by the common Pb correction. So, although the MSWD of the Concordia age is relatively large, the ages are considered realistic within the uncertainties given (Fig. 7).

Deformation and metamorphic history

The study area records polyphase deformation involving three generations of ductile structures comprising folds, foliations, and shear zones. Ductile shear zones locally grade into brittle or brittle–ductile structures, commonly associated with kinkbands and localized open to tight chevron folds. The penetrative structures (D_1–D_3) are described from old to young.

Early deformation (D_1 and D_2)

A composite transposition foliation (S_m) and a mineral/stretching lineation referred to as L_m/L_s (Figs. 3A, 3B, and 4F) represents the main L-S fabric in the gneisses and schists.

S_m is consistently folded by F_3 and is a composite of S_1 and S_2 on the limbs of F_2 isoclines (Figs. 4B and 4C). L_m is defined by minerals such as hornblende, sillimanite, kyanite, and mica, as well quartz and feldspar aggregates, which are parallel to a stretching lineation (L_s) defined by boudinage, strain shadows, quartz ribbons, and rodding (Figs. 3B and 4F). L_m/L_s comprises at least two generations of lineations (Fig. 4H). An old lineation interpreted to be related to D_{1-2} is folded by F_3 and commonly parallel to F_2 hinge lines (Fig. 4F), whereas a younger lineation is commonly parallel to F_3 hinge lines (Fig. 9). These lineations are difficult to separate where F_3 folds are absent or not well exposed. F_2 folds are tight to isoclinal, commonly intrafolial structures that refold rare isoclinal F_1 folds of compositional layering (Fig. 4A), generally into fishhook fold interference patterns (Fig. 4A). Despite the rarity of F_1, an S_1 schistosity or differentiated metamorphic layering is generally well developed in rocks of the PABC and GBC (Figs. 3G, 4B, and 4E). F_2 locally includes sheath folds (Fig. 4C).

Fig. 9. Lower hemisphere equal area projections of the structural elements in the GBC, PABC, and HLCG. First column present Sm, second column F3 and S3, and third column the colinear F2 and *Ls*/*L*m. Note that the F2 are generally parallel to the set of *Ls*/*L*m that is transverse to F3 (see text). Girdles represent the regional folding of Sm by F3 and the orientation of its axial surface (S3). Contouring at 2% intervals. PABC, Port aux Basques Complex; HLCG, Harbour Le Cou Group; GBC, Grand Bay Complex.
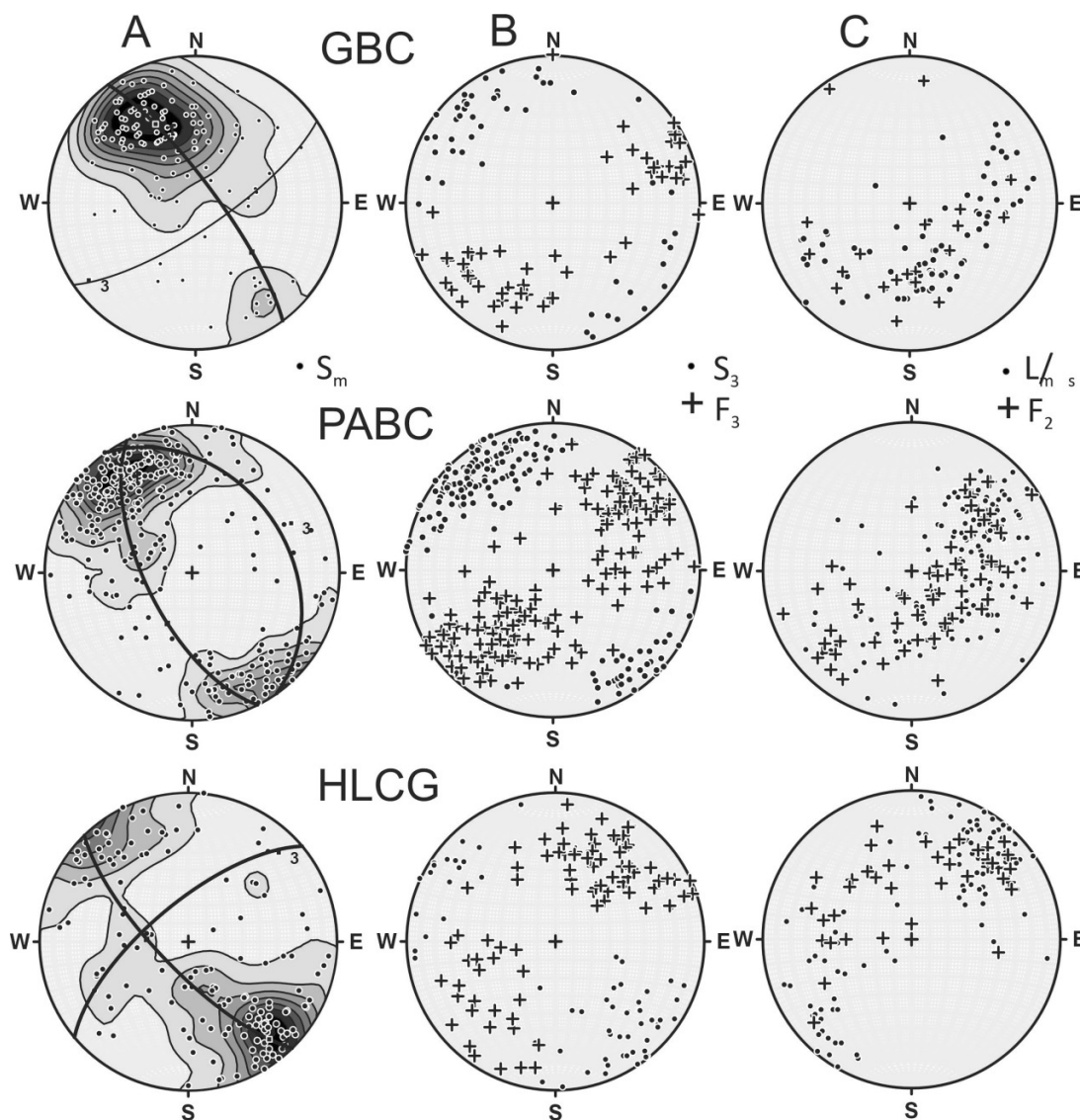
Peak metamorphic kyanite and garnet porphyroblasts grew over S_1 and are locally wrapped around by S_2 and S_3 with inclusion trails curving into S_2, indicating that peak metamorphism culminated immediately prior to and/or early during D_2 (Burgess et al. 1995). Kyanite lying in S_1 is locally folded by F_2 and F_3; kyanite folded by F_3 is partially or nearly completely altered to white mica. Garnet locally shows complex inclusion trails with textural unconformities and zonation. The oldest generation of garnet preserved as cores in zoned or as individual porphyroblasts with inclusion trails of quartz, opaque, and mica may have started to grow during D_1, as S_2 at a high angle to the inclusion trails wraps around these garnet porphyroblasts. Inclusion-free rims of zoned garnet around inclusion-rich cores locally grew across S_2 in pelitic schists indicating they also grew during and/or after D_2, but probably before D_3 because garnet in the hinges of open to tight F_3

microfolds are commonly strongly altered with chlorite-rich coronas and are wrapped around by S_3. Hence, D_1 and D_2 are inferred to have formed part of a continuum or a progressive deformation (Burgess et al. 1995).

Aplites and pegmatitic veins cut S_m and together with irregular granitoid leucosomes generated during in situ melting (Burgess et al. 1995) are folded by F_2 and F_3 (Figs. 4E and 5). One F_2- and/or F_3- folded white biotite granitic dike that cuts S_m in the Margaree orthogneiss yielded a U–Pb zircon age of $417\ ^{+7}/_{-4}$ Ma (Valverde-Vaquero et al. 2000), suggesting it is an offshoot of the Rose Blanche pluton (417 ± 2 Ma, Figs. 7, and 8). The relative age of the folds in this outcrop is ambiguous but provides a maximum age for the start of F_3. The Rose Blanche granite and its many offshoots in the HLCG locally cut S_2 but are also locally folded by F_2 (Fig. 3F), locally are parallel to the axial surfaces of F_2, and/or acquired a S_2 folia-

tion and lineation where the granite occurs as narrow sheets and/or was mylonitized (Fig. 6B). The granitoid veins are consistently folded by F_3 (van Staal et al. 1992; Lin et al. 1993; Benn et al. 1993), suggesting that the intrusion of the Rose Blanche granite in the HLCG overlapped with the final stages of D_2, but outlasted D_2 in other places. This is consistent with the microstructures. Fabrics in D_{1-2} shear zones marked by relict S-C and shearband foliations (Figs. 3E and 7B) and enhanced strain generally show a high degree of grain boundary area reduction that followed dynamic recrystallization. Evidence of the latter is locally preserved in orientation families of quartz and feldspar grains that outline once elongated grains. F_{1-2} folded or kinked micas (biotite and muscovite) and hornblende in differentiated foliation planes also show a high degree of recrystallization (Williams et al. 1977), although the microscopic fold hinges are commonly still recognizable. Combined all evidence suggest that high temperature was maintained after D_2 deformation largely had ceased in the rocks.

Late deformation (D_3)

F_3 folds are upright to steeply inclined, shallow to moderately plunging, generally non-cylindrical structures (Figs. 4B, 4D, 4E, 4G, and 4H), and occur throughout the GBC, PABC, HLCG, and Bay du Nord Group from microscopic to macroscopic scale, consistent with the girdles defined by the regional distribution of S_m (Fig. 9). F_3 folds are open to isoclinal buckle folds with near similar shapes (class 1 C-3) where the folds are tight (Figs. 4D and 4G) or less commonly near-isoclinal, indicating modification by superimposed strains into flattened folds. They are largely responsible for the northeast–southwest trending structural grain of the rocks in this area (Figs. 2 and 9). S_3 is a crenulation cleavage where F_3 defines tight folds of the main foliation (Fig. 4G), which in the GBC, PABC, and HBCG is a composite S_{1-2} foliation. F_3 is in places difficult to separate from F_2 where overprinting relationships are lacking, especially in zones of high D_3 strain such as the CRFZ and IMDZ. S_3 is generally well developed in schistose rocks, but locally absent or poorly developed where F_3 folds are open structures (Fig. 4B) and/or chevron folds. The average S_3 west of the IMDZ has a steep dip (ca. 70°–80°) towards the southeast (ca. 140°) (Figs. 5 and 9). S_3 has the same northeast–southwest strike east of the IMDZ in the HLCG, but the majority of the mesoscopic F_3 folds plunge moderately to shallowly towards the northeast (Figs. 6 and 9) generally overlapping the fields where a portion of the L_m/L_s and F_2 hinge lines plot. Kinked biotite and muscovite folded in F_3 show evidence of kinkband boundary migration (Williams et al. 1977) and some recrystallization and new growth of micas in S_3. However, contrary to the micas deformed by intrafolial F_2 folds, biotite folded and kinked in the hinges of F_3 together with garnet and hornblende is commonly partially altered to chlorite indicating that retrogression initiated during D_3. Furthermore, biotite, hornblende, and cummingtonite show undulose extinction and subgrains where folded by F_3, whereas feldspar and quartz locally still have irregular serrated grain boundaries indicating that recovery, grain-boundary area reduction, and recrystallization were not as prevalent during

D_3 as during D_{1-2}, which is also consistent with preservation of evidence for dynamic recrystallization defined by mantled porphyroclasts of microcline and plagioclase preserved in D_3-related shear zones. Hence D_3 probably postdated peak amphibolite facies metamorphism.

S_3 displays minor regional variations in strike (Fig. 9), which may be due to younger localized warping associated with the major shear zones. F_3 folds dominantly plunge shallowly to moderately to the southwest in the GBC and PABC but show a plunge reversal to northeast plunges in the eastern and northeastern part of the areas (Fig. 9), which produced large domal structures such as the Dolphin Road dome (Fig. 2). F_3 folds are generally overturned to the northwest consistent with steeply southeast-dipping S_3 in these areas. In contrast, the majority of mesoscopic F_3 folds plunge shallowly to the northeast in the HLCG colinear with the map scale, Grandy Sound F_3 antiform, which is slightly overturned to the southeast, consistent with the generally steep dip of S_3 to the northwest (Fig. 9) in this part of the HLCG. The sense of F_3 overturning is most prominent in the eastern part of the area underlain by the HLCG (Fig. 6). In the western part of the area near or within the IMDZ, S_3 fans from steeply southeast to steeply northwest dipping in the HLCG (Fig. 5).

F_3 folds rotated the older structures (S_m) into steeply dipping orientations, especially where they are penetrative tight structures such as near the IMDZ (Fig. 5). An exception is the core of the Grandys Sound antiform where the enveloping surface to S_m has a shallow dip (Figs. 3F and 4C). F_3 folds also fold the GRSZ (Fig. 5) and GBFZ (Figs. 2 and 10) that separate the HLCG and PABC and PABC and GBC, respectively, indicating the tectonites of these fault zones were subjected to a polyphase history. Preserved down-dip shear-sense indicators (Fig. 3A) in the tectonites probably formed during pre-D_3 shearing. D_3 consistently overprints the 417 ± 2 Ma Rose Blanche and 416 ± 4 Ma La Poile granites and related apophyses (Fig. 3E) consistent with microstructural evidence that it postdates peak amphibolite facies metamorphism.

Lineations and fold hinge lines

Two generations of linear structures are present in part of the rocks (Fig. 4h). The old generation of mineral/stretching lineations (L_m/L_s) is folded by F_3 (Fig. 4F) and locally also by F_2. These lineations generally have steep-to-moderate pitches, are defined by peak-metamorphic minerals (hornblende, kyanite, sillimanite, and cummingtonite), and have a trend at moderate-to-high angles to S_3. This transverse lineation is interpreted to have formed during D_{1-2} and as a rule is colinear or nearly so with F_{1-2} hinge lines (Fig. 8), suggesting the latter were progressively rotated into parallelism with L_m/L_s due to high non-coaxial D_{1-2} strains, consistent with the presence of F_2 sheath folds (Fig 4C). Sheath folds locally deform the L_m/L_s, but this is not apparent for most F_{1-2} folds. Some of these structures are reclined folds, or nearly so with straight hinge lines, which are referred to as curtain folds by Passchier and Trouw (2005). The second set of lineations generally has moderate-to-shallow pitches and is generally parallel to F_3 hinge lines (Fig. 4H), especially near D_3-related

Fig. 10. Tectonic models for Salinic (A) and Acadian (B) orogenies modified from van Staal and Barr (2012) and van Staal et al. (2014a). The sketches presented in A–E represent cross-sectional cartoons depicting the progression in tectonic settings from D1 to D3 of the collision between the Gander margin and composite Laurentia. (A) D1 (Salinic) underthrusting of the Gander margin (A-subduction) with shear localized in the GRSZ and folding and foliation development in the adjacent rocks; (B) D1 progressed into D2 structural thickening in the Salinic collision zone, which leads to folding of the GRSZ. Granite intrusion and peak temperature Barrovian metamorphism characterize the terminal stage of D2; (C) Post 417 Ma tectonic escape of a wedge of high-grade rocks towards the southeast such that the HLCG is thrust over the BDNG. The tectonites preserved between the CRFZ and GBFZ accommodated pre-D3 normal sense of motion with respect to their hangingwall, which is now inferred to be buried beneath the leading western edge of the Meelpaeg structure; (D) Early stage of D3 (Acadian) bi-vergent Meelpage structure development with reverse shear strain localized in shear zones such as the CRFZ and BMFZ. Northwestward-dipping D2 tectonites involved in the preceding tectonic escape between the CRFZ and GBFZ progressively rotate and acquire a southeasterly dip; (E) F3 folding and progressive D3 steepening of the shear zones formed during Meelpaeg structure formation. The steepened shear zones acquire a favourable orientation to accommodate dextral strike–slip motions. The timing of the various stages is approximate and/or interpretative, and in part based on existing constraints concerning the start and end of the Salinic collision in southern Newfoundland (see text). Most abbreviations are given in text and previous figures. BB, Badger–Botwood basin; BA, backarc to coastal arc (CA); BEF, Bay d'Est Fault; FA, forearc to coastal arc; ORS, Old Red Sandstone and related terrestrial rocks in red, which become progressively younger southeastwards; RRB, Rocky Ridge basin; VA, Victoria arc; WPG, Windsor Point Group.
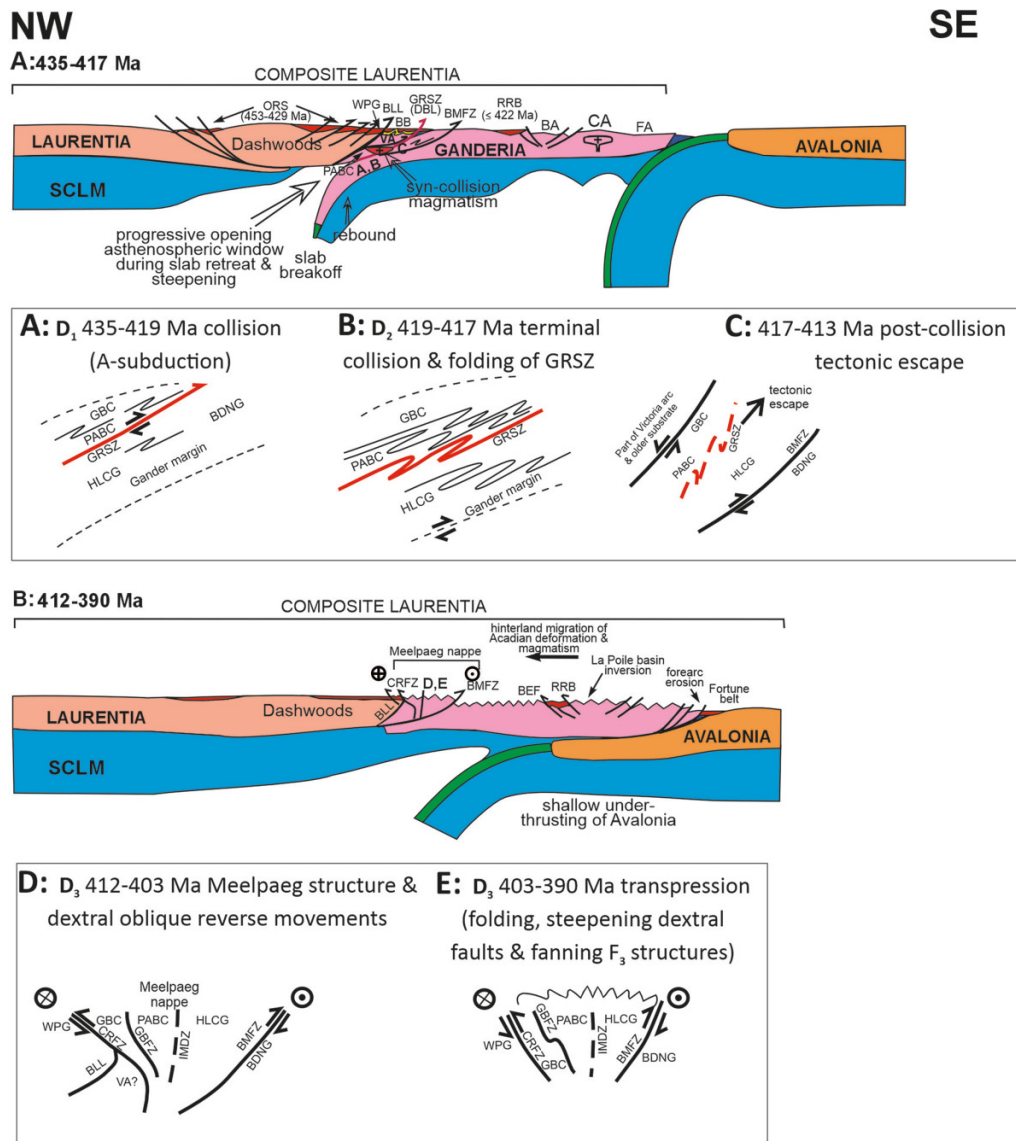
shear zones where it becomes the dominant lineation (e.g., Benn et al. 1993; Lin et al. 1993). In part this lineation may be defined by high-grade metamorphic minerals (Burgess et al. 1995), which in many places impeded direct assessments of their relative structural age in the field. However, sillimanite is commonly folded and crenulated by F_3 when examined in thin section and hence microstructural relationships are important separating D_{1-2} from D_3 and younger linear structures. The older lineation is progressively obscured, modified, and/or destroyed where the post-D_2 strain increases near D_3-related shear zones (Benn et al. 1993, see below), consistent with scarcity of transverse lineations in the major fault zones (Figs. 5 and 6). The lineation set with moderate-to-shallow pitches, trending (sub)parallel to S_3 and F_3 hinge lines, thus likely formed during D_3 and/or during subsequent strike–slip-related shearing. It locally may have involved rotation of the older lineation set (with steeper pitches), particularly in straight gneiss and mylonites that accommodated a component of strike–slip shear. Hence, the relative age of the lineation in a rock is difficult to establish in the field where overprinting relationships are absent between folds and lineations and thin sections are unavailable.

L_m/L_s displays a large spread between northeast and southwest in a girdle that lies in S_m in the GBC and PABC, with few if any plunging to the west or northwest (Fig. 9). The opposite is shown in the HLCG where the lineations also have a similar spread between northeast and southwest, but none is plunging to the southeast. Instead, the lineations with steep pitches plunge to the west or northwest. This difference reflects the reorientation of S_m during regional folding by F_3 folds, which are generally overturned to the northwest in the GBC and PABC, whereas they are generally overturned to the southeast in the HLCG. This relationship is consistent with the other lines of structural evidence that suggest the lineation set with steep pitches formed before D_3.

Shear zones and age of deformation

The area is dissected by several major wide shear zones that also define the structural boundaries between the four tectonostratigraphic units discussed herein. These shear zones are characterized by zones of enhanced strain represented by banded mylonites in quartzofeldspathic gneiss (straight gneiss sensu; Hanmer 1988) and phyllonites in phyllosilicate-rich rocks, and the presence of shear sense indicators (Figs. 3A, 3E, 3G, and 6). These shear zones commonly preserve evidence of a long history of movements and progressive strain localization culminating in brittle–ductile faults and cataclasites (Figs. 3C and 5C). Local folding of the mylonites and/or strands of the shear zones by F_2 and/or F_3 folds (Figs. 2, 5, and 10) attest to their longevity.

Cape Ray Fault zone and associated fault zones in the Grand Bay Complex

The CRFZ is a steeply southeast-dipping structure (Fig. 2B) that separates the Upper Ordovician to Silurian (sub)greenschist grade rocks of the largely terrestrial Windsor Point Group, which lies unconformably on Ordovician

arc rocks of the peri-Laurentian Dashwoods terrane in the footwall (Dubé et al. 1996; van Staal et al. 2007), from the highly strained amphibolite facies gneissic tectonites of the GBC in the hangingwall. It also represents the basal shear zone of the western edge of the Meelpaeg structure (Fig. 1). The Windsor Point Group is mylonitized over a width of ca. 500 m. (Dubé and Lauzière 1996) and banded mylonites and phyllonites in the GBC have a width of 1–2 km east of the structural contact with the Windsor Point Group, but kinematically related shear zones characterized by enhanced strain, such as the Big Barachois fault (Fig. 2), and shear–sense indicators occur throughout the GBC further to the east (Figs. 2B, and 3D) (van Staal et al. 1992). Mineral lineations and F_2 hinge lines are parallel to a stretching lineation defined by boudinage, strain shadows, ribbons, and rodding in the mylonites and other tectonites, which plunges dominantly between southwest and southeast (Fig. 9). The movement history of the CRFZ is complex and comprises several kinematically distinct phases (Dubé and Lauzière 1996), which may reflect different tectonic events (see below).

The dominant phase of shearing accommodated dextral reverse motion, which inverted the older metamorphic zonation in the GBC near the CRFZ (Fig. 2B) and culminated in progressive retrogression of the amphibolite facies tectonites of the GBC to greenschist-facies phyllonites and mylonites (Dubé and Lauzière 1996). This phase of shear occurred after peak amphibolite facies metamorphism, which occurred before and/or during intrusion of the late syn-D_2 Rose Blanche granite (417 ± 2 Ma, Fig. 7). Early Devonian U–Pb titanite ages ranging between 412 (Dunning et al. 1990) and 405 Ma (Figs. 2, 7, and 8) and $^{40}Ar/^{39}Ar$ hornblende ages of 407 to 402 Ma (Dubé et al. 1996) in the retrogressed GBC mylonites (Fig. 2) associated with the CRFZ and related faults such as the Big Barachois fault and GBFZ suggest the west-directed phase of dextral oblique reverse shearing probably started no earlier than 412 Ma and mainly took place in the early Emsian. In addition, the ductile reverse shear zones locally transgressed into brittle–ductile or brittle reverse faults (Fig. 3C) emphasizing that this progressive deformation was probably accompanied by significant denudation during uplift of the GBC with respect to the Upper Ordovician to Silurian conglomerates and clastic rocks of the Windsor Point Group. Greenschist facies muscovite in tectonites of the Rose Blanche granite associated with horizontal dextral sheared rocks where the granite is truncated by the CRFZ in the northwest (Fig. 1) yielded late Emsian K–Ar ages of 403–399 Ma (Dubé et al. 1996), whereas subsequent, more localized dextral strike–slip was cut by the ca. 384 Ma Strawberry granite (Fig. 2), indicating that dextral kinematics remained active in the CRFZ until the Middle Devonian. F_3 locally not only folds the CRFZ mylonites and associated stretching and mineral lineations (S_m/L_m), but also becomes tighter towards the CRFZ. F_3 axial planes locally curve into parallelism with the mylonites (Fig. 3G) and S_3 is overprinted by dextral shear bands. Hence F_3, at least in part, overlapped with the west-directed oblique shearing associated with the CRFZ and related fault zones. Dextral shearing and F_3 folding are therefore grouped together in D_3. The degree of overprint and reorientation of the main S_m/L_m fabric during the complex dextral oblique reverse shearing

and F$_3$ is difficult to gauge but may be substantial and hence cannot be used here to constrain the kinematics associated with earlier movements related to D$_{1-2}$. D$_3$ postdates the Rose Blanche and La Poile granites (Figs. 2 and 7) and thus occurred in the Devonian and represents structures related to the Acadian orogeny. Dextral transcurrent movements in turn were locally followed by minor sinistral strike–slip motion after ca. 384 Ma (Dubé and Lauzière 1996). Various generations of kinkbands and localized chevron folds formed during both phases of strike–slip motion. Overprinting relationships between these structures are commonly ambiguous and irrelevant for this study and hence not discussed in any detail herein. They are all grouped under D$_3$.

Grand Bay Fault zone (GBFZ)

The southeast-dipping GBFZ can be traced as a lineament along the boundary between the GBC and the PABC for several kilometres, although the fault zone is only locally exposed. It separates the inferred Cambrian to Floian PABC from the structurally underlying rocks of the GBC (Figs. 2B and 10), which are inferred to be Floian to Dapingian (see above), suggesting an "old over young" geometry across the fault. The fault zone is only well exposed in a few places along its strike length, but mylonites and banded straight gneiss with dextral oblique reverse shear sense indicators, as in the CRFZ, occur in several outcrops north and south of the Trans Canada Highway immediately west of the town of Port aux Basques. Small-scale ductile or ductile–brittle thrust zones occur in its footwall (Fig. 3D). The shear zone tectonites locally truncate or overprint the main composite foliation (Sm) and F$_2$ folds, hence the fault is mainly a relatively late structure that formed after D$_2$. Regional mapping suggests that this structure follows a band of Kelby Cove orthogneiss that defines the boundary between the GBC and PABC (Figs. 2 and 10), which was folded by large doubly plunging F$_3$ folds in a geometry like shown in Fig. 4D. The GBFZ and the nearby Big Barachois fault (Fig. 2) probably had complex movement histories, but the dextral oblique reverse motion is grouped with D$_3$. The shearing started early, before any significant F$_3$ folding, and continued afterwards. U–Pb titanite from banded gneiss immediately adjacent to and/or in the GBFZ yielded ages of 410 and 405 Ma, respectively (Figs. 2 and 7), which we interpret as crystallization ages (Hartnady et al. 2019) associated with prolonged D$_3$-related strain and retrogressive amphibolite facies metamorphism localized in the shear zone.

Isle aux Morts deformation zone (IMDZ)

The IMDZ (Fig. 5) comprises an important but complex zone, 0.5–2 km wide, of enhanced strain comprising sheared tectonites and cataclasites of the PABC and HLCG situated between the discrete Isle aux Morts and Otter Bay faults. The latter two structures are outlined by lineaments on airphotos and are characterized by narrow zones of ductile–brittle shear zones and/or cataclasite (Fig. 5C) commonly with dextral kinematics where exposed. Tight to isoclinal folds, marked attenuation and boudinage, and an abundance of shear sense indicators (Figs. 3E and 3H) characterize this zone of enhanced strain. The Isle aux Mort fault truncates the main

ductile shear zone (GRSZ), which is localized in a thin, continuous band (10–50 m thick) of ca. 451 Ma (Fig. 7) highly tectonized Port aux Basques granite (Figs. 3H, 5A, and 5B), a few kilometres northeast of the village of Isle aux Morts (Figs. 1 and 2). The GRSZ is complexly folded by F$_2$ (Burnt Island Brook structure) and F$_3$ (Fig. 5A) and defines the tectonic boundary between the PABC and HLCG. The distinctive Port aux Basques granite and Margaree orthogneiss of the PABC are absent in the HLCG (Fig. 2). The sheared, narrow band of Port aux Basques granite (Fig. 3H) tectonites extends continuously for more than 20 km and consistently separates the HLCG from the PABC (van Staal et al. 1996b). The two units differ markedly in their lithological make-up and Ordovician tectonomagmatic history, indicating the GRSZ marks a major pre-D$_2$ tectonostratigraphic boundary (Fig. 10) that juxtaposed unrelated units. The tectonostratigraphic contrasts are typical of the Dog Bay Line (Williams et al. 1993), which separates elements of the Victoria arc and Exploits backarc basin (Zagorevski et al. 2010) characterized by an abundance of magmatic rocks interpreted to have formed in these settings (Margaree and Kelby cove orthogneisses), from the adjacent coeval sediment-dominated successions with rare volcanic rocks related to rifting associated with backarc opening (Schofield et al. 1998); hence the GRSZ represents an along strike segment of this structure that was overprinted and translated during formation of the Meelpaeg structure (Fig. 10A, stage C). The two bounding fault strands (Fig. 5A) of the IMDZ thus envelope a lenticular zone of sheared PABC and HLCG rocks that widens to the northeast until the movement zone is cut by the ca. 417 Ma Rose Blanche granite to the northeast (Fig. 1). Hence the GRSZ was active between 451 and 417 Ma, thus mainly during the Silurian Salinic orogeny, considering the Upper Ordovician Port aux Basques granite formed before D$_1$ and that the Rose Blanche granite intruded late during D$_2$. However, continuation of narrow dextral shear zones within the Rose Blanche granite, along strike of the western Isle aux Mort fault, indicates dextral movements were accommodated in the IMDZ during the Early Devonian (Fig. 1). The movement history of the rocks in the IMDZ is complex like that preserved in the CRFZ and BMFZ (see below), recording both early reverse (Fig. 3A), sinistral and later dextral horizontal movements (Fig. 3G) according to shear–sense indicators (e.g., shearbands, C-S fabrics, asymmetrical boudinage, etc.; van Staal et al. 1992). Macroscopic folding of the GRSZ tectonites by F$_2$ and F$_3$ in the Burnt Island Brook structure (Fig. 5) indicate that shearing must have started prior to F$_2$ when S$_m$ probably was shallowly dipping considering the generally shallow plunges of the upright F$_3$ folds (Fig. 9). Kinematic interpretations of folded shear zones are thus dependent on restoring them to their pre-folding attitudes.

Bay Le Moine Fault zone (BMFZ)

The BMFZ (Fig. 6A) is a northeast-trending curviplanar structure, several kilometres wide, comprising both ductile shear zones and brittle fault strands that combined separate the upper amphibolite facies rocks of the HLCG from the greenschist facies rocks of the lithologically similar Bay du

Nord Group (Lin et al. 1993) to the east. The main ductile shear zone is ca. 1 km wide and the juxtaposed rocks were subjected to an identical structural history on both sides of the fault (Lin et al. 1993; van Staal et al. 1996b). Hence, this fault zone is not an important tectonostratigraphic boundary like the GRSZ, but merely a major fault zone that separates rocks of the same tectonostratigraphic unit at different metamorphic grades. Its movement history is complex involving both sinistral and dextral shear (Lin et al. 1993), which both affect the Rose Blanche granite, but the non-coaxial shear–sense indicators formed during the younger dextral phase are restricted to the main shear zone, whereas the older sinistral shear indicators occur over a wider area. Small-scale F_3 folds in the BMFZ are consistently dextral, which combined with the clockwise sense of rotation of their curviplanar fold axial surfaces and axes indicate that an important phase of ductile dextral shearing was associated with D_3. F_3 folds deform S_2 in the adjacent Rose Blanche granite and its migmatitic envelope (Figs. 2 and 6) indicating that D_3 and the associated dextral shear occurred during the Early Devonian Acadian orogeny as in the PABC and CRFZ. The onset of dextral shearing, however, is poorly constrained by our data set, because shearing may have started as early as the final increments of D_2, during or shortly after intrusion of late Rose Blanche granite-related aplites, which cut S_m but were sheared dextrally (Fig. 6B), although this contradicts other observations that sinistral shear was active during Rose Blanche magmatism (see below). The onset of D_3 likely happened after intrusion of the ca. 416 Ma distinct megacrystic La Poile granite (Chorlton 1980; Chorlton and Dallmeyer 1986), which was juxtaposed with the more penetratively deformed Rose Blanche granite by the BMFZ and deformed during D_3. La Poile granite offshoots that had intruded the Rose Blanche pluton near to and within the BMFZ cut S_m and were sheared dextrally and/or folded during D_3, although the overall strain is commonly less than in the Rose Blanche granite. The ca. 416 Ma La Poile granite thus postdates D_2 and predates D_3 (=D_2 of Chorlton and Dallmeyer 1986). The BMFZ cuts and widens into both granites further to the north (Fig. 1). Dextral shearing thus mainly occurred during the Early Devonian, which is consistent with the observation that the ductile segment of the BMFZ is cut by the ca. 397 Ma Petites granite (Kerr et al. 2009), which in turn shows a ca. 2.8 km dextral offset (Fig. 6) during later, mainly brittle movements (Lin et al. 1993). D_3 thus overlapped with dextral shearing, as in the CRFZ. Stretching lineations in the BMFZ and immediately surrounding tectonites dominantly have shallow to moderate westerly to southwesterly plunges (Fig. 6), suggesting the shear zone accommodated both horizontal and vertical movements, such that the greenschist facies rocks of the Bay du Nord Group moved downwards with respect to the amphibolite facies rocks of the HLCG. The sinistral shear sense indicators in tectonites that occur within or adjacent to the BMFZ are associated with transverse NW–plunging lineations (Fig. 9) and probably accommodated an important increment of reverse motion prior to D_3 dextral shear. We tentatively interpret the wider zone of west-dipping tectonites adjacent to the BMFZ as having accommodated oblique sinistral reverse shear during and possibly shortly after D_{1-2} but before D_3.

Sinistral oblique shear lasted at least until intrusion of the Rose Blanche granite since sinistral shear locally overprints granite offshoots (Fig. 3E) and aplites show clear syntectonic relationships in several places. Contradictory syntectonic relationships displayed by aplites in dextral mylonites (Fig. 6B) could be reconciled if a switch from sinistral to dextral shear occurred late during or immediately after Rose Blanche intrusion. Regardless, both senses of shear suggest that some degree of tectonic transport of high-grade rocks of the HLBC above the lower grade rocks of the Bay du Nord Group (Fig. 10C) was initiated during the early Lochkovian.

Metamorphism and age of deformation

The overall grade of metamorphism increases from northwest to southeast with the highest pressure and lowest temperature rocks occurring in the least retrogressed parts of the GBC and adjacent PABC (Figs. 2 and 8), which record growth of biotite, hornblende, kyanite, staurolite, and garnet before and early during D_2 (Burgess et al. 1995). Further eastwards in the PABC, modal staurolite decreases concomitantly with increase of modal kyanite, followed by introduction of anatectic melts in the kyanite zone, and subsequently followed by crystallization of sillimanite at expense of kyanite further to the east. In the eastern part of the PABC and HLCG the highest-grade pelitic and semi-pelitic rocks are characterized by sillimanite, garnet and K-feldspar-bearing assemblages and show a marked increase in the degree of migmatization. Hornblende in the garnet amphibolites becomes progressively browner with increasing metamorphic grade and amphibolites show an increase in the modal content of clinopyroxene. The progressive increase in peak metamorphic grade from northwest to southeast without evidence for a metamorphic break between the PABC and the HLCG across the GRSZ (Figs. 2 and 8) suggest that the metamorphic isograds and the enveloping surface to the D_{1-2} structures have an overall northwesterly tilt, which was created late during or after D_2. Pressure–temperature conditions varied from c. 600–650 °C in the west to 700–750 °C in the east. Pressures ranged between 10 and 8 kb (Burgess et al. 1995). Migmatization culminates in a wide envelop of strongly migmatized pelitic and semi-pelitic rocks around the Rose Blanche granite body (van Staal et al. 1996b), suggesting that peak high-T metamorphism in the HLCG was achieved close to the time of intrusion, consistent with the 418 ± 9 Ma U–Pb titanite and 419 ± 2 Ma ^{39}Ar/^{40}Ar hornblende ages in the HLCG (Figs. 2 and 8), which overlap in error with the preliminary 417 ± 2 Ma U–Pb zircon age of the Rose Blanche granite (Figs. 7 and 8). The 418 ± 9 Ma titanite is a ^{206}Pb/^{207}Pb age from a migmatitic gneiss of the Otter Bay Formation in the relatively low-strain hinge of the F_3 Grandy Sound antiform (Fig. 2), suggesting that the titanite age relates to late syn-D_2 peak metamorphism, which is consistent with the ^{206}Pb/^{238}U and ^{207}Pb/^{235}U ages, which are both 420 ± 2 Ma (Burgess et al. 1995). The age of the Rose Blanche granite is preliminary but may be as old as 419 Ma (Devonian–Silurian boundary; Cohen et al. 2022), which is consistent with an unpublished SHRIMP age of ca. 419 Ma (C. Wang, written communication (2023)). Hence, the metamorphism associated with structural burial ($\sim$10 Kb)

during D_1 to early D_2 based on the relative age of growth of kyanite and garnet porphyroblasts (see above), probably occurred before peak-temperature Barrovian metamorphism at ca. 8 Kb (Burgess et al. 1995), near the Silurian–Devonian boundary or earlier.

The onset of D_3 likely started after intrusion of the ca. 416 Ma La Poile granite (Chorlton and Dallmeyer 1986), but before the greenschist facies conditions, which were reached between 403 and 390 Ma as indicated by the Ar ages of biotite and muscovite (Fig. 8) in tectonites of the CRFZ and IMDZ (Fig. 2), which were both active during D_3 (Figs. 2 and 10). This interpretation is consistent with titanite ages in D_3-related shear zones between 412 and 405 Ma (Figs. 2, 7, and 8), which are interpreted as (re)crystallization ages (Hartnady et al. 2019) during D_3. Four U–Pb monazite ages in migmatitic tectonites of the PABC and HLCG range from 416 to 413 Ma (Fig. 8), regardless of whether they are proximal or distal to D_3 shear zones (Fig. 2). The oldest monazite ages of ca. 416 Ma overlap in error with the age of the Rose Blanche granite and may have grown during peak-temperature metamorphism, whereas the two slightly younger ages could record new growth and/or recrystallization during retrograde amphibolite facies metamorphism associated with increments of early exhumation (see below) during the Lochkovian before the onset of D_3 (Fig. 8). New growth and/or recrystallization of monazite is common in collisional orogens (Martin et al. 2007), evidenced by the growth of ca. 404 Ma monazite in the Port aux Basques granite tectonite that defines the GRSZ (Fig. 7). Combining all available age constraints (Figs. 2 and 8), particularly the dated titanites of D_3 related tectonites, we infer that D_3-related shearing started after 412 Ma and continued until the Middle Devonian.

Macroscopic structure

The orientations of the main composite foliation (S_m), mineral/stretching lineation (L_m/L_S) and the F_3 hinge lines display significant variation in the investigated area (Fig. 9). L_m/L_s displays large spreads between northeast and southwest in girdles that lie in S_m. Girdles of S_m reflect folding by southwest- or northeast-plunging F_3 folds. The pole of the girdle of S_m coincides with the dominant southwesterly plunge of the measured mesoscopic F_3 folds in the GBC (Fig. 9). Mesoscopic and macroscopic F_3 folds generally show a plunge reversal to northeast plunges in the eastern and northeastern part of the investigated area especially in the eastern part of the PABC near the IAMDZ, creating elongated doubly plunging domal structures, well outlined by sheets of Port aux Basques granite and narrow bands of orthogneiss (Fig. 2). As a result, the distribution of S_m in the PABC defines two girdles, the poles of which coincide with the bimodal distribution of the hinge lines of mesoscopic F_3 folds, which plunge either to the northeast or southwest (Fig. 9). The average S_3 has a steep dip (c. 60°–80°) towards the southeast (c. 140°) west of the IMDZ (Fig. 9). S_3 has the same northeast–southwest strike in the HLCG east of the IMDZ but dips dominantly towards the northwest instead. S_3 thus fans from west to east. Towards the east, it first progressively steepens culminating with nearly vertical

or steep NW-dips in the PABC near to and within the IMDZ and then acquires dips towards the northwest in the HLCG. In addition, the majority of the F_3 folds in the HLCG plunge moderately to shallowly towards the northeast (Fig. 9). The girdle defined by S_m in the HLCG is a proxy for the orientation of the Grandy Sound antiform defined by the regional distribution of the two lithological formations in the HLCG (Fig. 2). The Grandy Sound antiform has a shallow (ca. 15°) plunge towards the northeast (048°), whereas its axial plane has a steep dip (ca. 73°) to the northwest (318°) using the girdle of S_m and mean orientation of S_3 in the HLCG (Fig. 9). The Grandy Sound antiform is cored by the older Otter Bay Formation (Fig. 2) and is thus an anticline macroscopically. Hence, the stratigraphy of the HLCG was structurally not inverted on a regional scale prior to D_3. The geometry of the F_3 structures with a changing vergence from northwest to southeast between the CRFZ and the BMFZ defines a fanning structure (Fig. 10B, stage D), associated with dextral shearing in the bounding fault zones.

Fold interference structures

The distribution of the Otter Bay and Grandy's formations in the HLCG suggests that the large F_3 Grandy Sound anticline and parasitic folds locally refold smaller scale F_2 folds (Fig. 2C), although in several cases the exact geometries of the interference patterns either could not be determined due to the unknown continuation of the units beyond the coastline or were not structurally analysed in detail. One exception is the Burnt Island Brook structure, which is defined by the narrow sheet of Port aux Basques granite that outlines the GRSZ along the boundary between the PABC and the HLCG (Fig. 5). Mesoscopic F_2 folds are overturned, recumbent, or reclined (Figs. 3F and 4C) in the core of the Grandy Sound anticline (Fig. 3F) and smaller scale F_3 folds (Fig. 2C), suggesting that the D_{1-2} structures had a shallow-to-moderate dip prior to F_3 folding, consistent with the moderate-to-shallow plunges of F_3 throughout the area.

Burnt Island Brook structure

The Burnt Island Brook structure is a fishhook-like fold interference pattern within the IMDZ. The interference pattern is defined by a large refolded asymmetrical S-shaped isoclinal F_2 fold and slightly more open northeast-trending F_3 folds (Figs. 5A and 5B). The hinge lines of the F_2 folds are parallel to the northeast-trending stretching lineations in the IDMZ (Fig. 5). The interference pattern is outlined by the well exposed (visible on-air photos) narrow band of Port aux Basques granite tectonite (Fig. 3H), but it is significant that similar interference structures involving the same rocks are commonly present on mesoscale as well (Fig. 4E). The Port aux Basques granite tectonite that defines the GRSZ comprises several individual narrow bands of granite, which are intimately interleaved with thin screens of highly strained amphibolite and migmatitic garnet and sillimanite-bearing semi-pelitic schist and gneiss of the PABC. The GRSZ tectonites are typically strained into straight gneiss and contains intrafolial F_2 folds of a well-developed S_1 (Fig. 3H), which are both folded by F_3 on all scales. Some of the Port aux Basques granite bands de-

fine shallowly doubly plunging domal-shaped structures with M-shaped mesoscopic F_3 folds in the hinge (Fig. 5). The domal structures highlights the curvilinear nature of F_3 (Figs. 4D, 4H, and 10C), although most F_3 folds have a shallow-to-moderate plunge to the northeast or north (Fig. 5). Grading in metasandstone beds and the distribution of coticule layers in the Grandy's Formation (Fig. 4D) indicate that the most northerly hinge of the refolded S-shaped F_2 isocline is an anticline with the Otter Bay Formation of the HLCG in its core.

Unfolding F_3 folds and tectonic transport

Interpretation of the distribution of L_m/L_s in the Meelpaeg tectonites of the Port aux Basques area is complicated because the relative age of a part of the measured lineations is ambiguous and the tight F_3 folds commonly have near similar shapes (Figs. 4G and H) in zones of enhanced strain, indicating various degrees of modification (flattening) of the buckle folds by superimposed strains, factors which hamper any in-depth interpretation of the lineation patterns (see Ramsay 1967). Unfolding of the shallow northeast plunging macroscopic F_3 folds suggests that both limbs of the F_2 Burnt Island Brook structure within the IMDZ (Fig. 5) were dipping to the north and hence this fold was overturned towards the south prior to F_3 refolding. The transverse set of L_m/L_s with steep pitches outside the zones of enhanced D_3 strain, inferred to be related to D_{1-2}, has an approximate trend between north and west when unfolded. Combining the restored attitudes of these two structures suggests that tectonic transport was directed towards an orientation between south and east before D_3, assuming the hinge lines of the Burnt Island Brook structure and associated parasitic F_2 folds in the IMDZ, which are parallel or nearly so to F_3 (Fig. 5), initially formed at a high angle to the transverse set of L_m/L_s and were progressively rotated into parallelism with the finite stretching lineation and F_3 in the IMDZ, due to high strains late during and after D_2. Such a movement picture is consistent with the structures displayed by Rose Blanche aplite veins in the hinge of a nearly upright, relatively open, shallowly plunging F_3 antiform (Fig. 3F) west of the IMDZ, where S_m was probably little reoriented during D_3. If the granite aplites are inferred to have intruded into sites oriented at a high angle to the infinitesimal extension direction, the orientation of the strain axes with respect to S_m, determined from the folded and obliquely extended aplite veins suggests the shear was directed towards the southeast. Considering the major contrasts in tectonostratigraphic and magmatic histories between the PABC and HLCG and the interpretation that D_{1-2} was a progressive deformation, the GRSZ probably accommodated thrusting of the PABC above the HLCG, which must have occurred before F_2 folding. D_{1-2} movements characterized by southeast-directed flow is consistent with the overall northwest tilt of the metamorphic isograds, and attenuation of the Grandy's Formation of the HLCG along the western limb of the Grandy Sound anticline where the unit is highly thinned and/or truncated along the GRSZ (Fig. 2).

Structural interpretations

Salinic deformation (D_{1-2})

There are few data to constrain the nature of D_1. It produced a penetrative foliation (S_1) of varying intensity in all rocks and folds (F_1) at mesoscale (Fig. 4A), although no map-scale folds of this generation have been recognized. Nevertheless, the growth of metamorphic minerals prior to F_2 (Burgess et al. 1995) suggest that the D_1 deformation must have led to significant structural burial, while F_2 folding of the GRSZ implies pre-F_2 emplacement of the PABC and GBC above the HLCG along this shear zone. The shear zone tectonites are strongly foliated mylonites and straight gneiss and contain numerous intrafolial isoclinal folds (Fig. 3H), suggesting they accommodated high strains compared to the enveloping rocks. D_{1-2} is inferred to have been associated with south- or southeast-directed tectonic transport involving thrusting and overturned folding based on the assumption that D_1 and D_2 formed part of a progressive deformation as suggested by the growth of metamorphic porphyroblasts relative to structure (Burgess et al. 1995). D_3-related folding and steepening of the shallowly dipping L-S tectonites formed during D_{1-2}, into steeply northwest-dipping attitudes in the HLCG would result in sinistral oblique reverse shear sense indicators (Fig. 3E) and moderate to steeply northwest plunging stretching lineations. Indications of map-scale F_2 folds are evident in the HLCG and shown in the cross-section (Fig. 2C). Taken together, the D_{1-2} tectonites are inferred to have been incorporated in a south- or southeast-facing orogenic wedge, which initially formed by progressive Salinic underthrusting (A-subduction) of the Gander margin (Fig. 10A, stage A) beneath composite Laurentia (van Staal 1994; Valverde-Vaquero et al. 2006). F_2 folding of the GRSZ suggest that closure of the Exploits backarc basin probably occurred during D_1 with south or southeast-directed tectonic transport continuing during the ongoing collision represented by D_2. Remnants of the rifted Victoria arc (PABC and GBC), isolated in the backarc basin during multiple phases of arc-rifting and disorganized spreading (Zagorevski et al. 2010), were also accreted and incorporated in the orogenic wedge (Fig. 10A, stages A and B). A comparable Salinic tectonic evolution, including southerly overturned F_{1-2} folds, was recognized in the Bay du Nord and Baie d'Espoir groups elsewhere (Blackwood 1983, 1984; O'Brien 1988), and in correlative rocks in New Brunswick where pieces of the rifted Popelogan arc (equivalent of Victoria arc) that became isolated in the Tetagouche backarc basin (=equivalent of the Exploits backarc) were pulled down the subduction zone and metamorphosed to high-pressure low-temperature metamorphism during D_1 (van Staal et al. 2008).

Acadian deformation (D_3)

Final emplacement of the Meelpaeg tectonites and their contained Rose Blanche granite above lower grade rocks occurred during D_3. The onset of shearing in the CRFZ arose at or shortly after 412 Ma based on Early Devonian U–Pb titanite and $^{40}Ar/^{39}Ar$ hornblende and biotite ages (Dunning et al. 1990; Dubé et al. 1996, this study) in the GBC tectonites between the CRFZ and GBFZ (Figs. 2 and 8), whereas

D$_3$-related shearing in the BMFZ occurred after intrusion of the ca. 416 Ma La Poile granite. Reverse tectonic transport along the CRFZ was in a westerly direction and associated with major retrogression to lower greenschist facies conditions in the hanging wall rocks (Dubé and Lauzière 1996), but towards the southeast along the BMFZ (Lin et al. 1993) (Fig. 10B, stage D). The "Meelpaeg nappe" of Valverde-Vaquero et al. (2006) is thus neither a klippe nor a single thrust nappe, but a bi-vergent structure comprising two major thrusts with opposite sense of dip–slip motions. Structural evidence discussed earlier (see CRFZ section) suggests that F$_3$ folding and dextral-reverse shearing, at least in part, overlapped in time. Hence, the penetrative horizontal shortening of the Meelpaeg tectonites by F$_3$ folds also probably caused steepening of the CRFZ and BMFZ (Figs. 2B, and 10B stage E). In addition, the presence of F$_3$ folds throughout the tectonites that define the CRFZ and BMFZ and large-scale F$_3$ folds of the GBFZ and Big Barachois fault (Fig. 2) indicate that west-directed tectonic transport had started before significant F$_3$ folding, thus when the fault zones had shallower dips. The same relationships were observed near the Victoria Lake shear zone (Fig. 1, VLSZ), which represents the continuation of the CRFZ to the northeast (Valverde-Vaquero et al. 2006). Reverse bi-vergent tectonic transport of the Meelpaeg tectonites is thus interpreted to have started early during D$_3$, before penetrative regional F$_3$ folding. Hence, the regional fanning of S$_3$ from east to west between the moderately to steeply southeast-dipping CRFZ in the west and the steeply NW-dipping BMFZ in the east, which resembles the geometry of a ductile positive flower structure if the presence of F$_3$ folds is ignored, probably formed relatively late during D$_3$ (Fig. 10B, stage D). Steepening of the earlier bi-vergent reverse faults during F$_3$ folding progressively rotated them into steep orientations favourable for accommodating late dextral strike–slip motions, which is consistent with the parallelism between the shallowly plunging stretching lineations and F$_3$ hinge lines near the major fault zones (Fig. 9). D$_3$ culminated into formation of narrow brittle faults (Figs. 3C and 5C) after 397 Ma, which continued until at least the Middle Devonian. D$_3$ thus represents a complex, protracted dextral transpressive deformation system, which culminated with the juxtaposition of the upper amphibolite facies rocks (8–10 kb) with lower grade greenschist or sub greenschist facies rocks on each side of the bi-vergent structure.

Regional structural correlations with other parts of the gander margin in Newfoundland

The composite Gander margin shows a remarkable consistent evolution in structural style from northeast to southwest Newfoundland, although there may be differences in the number of fold generations recognized from one locality to the other, duration of the sense of shear and diachroneity in development of structures. South- or southeasterly overturned or recumbent structures are refolded by northeast-striking steeply inclined or upright F$_3$ folds and/or northwest-directed reverse faults of various intensities along the length of the margin in eastern (e.g., Holdsworth 1994) and southern Newfoundland (Blackwood 1983, 1984; O'Brien 1988; O'Brien et al. 1993) where the structural grain commonly has a more East–West strike.

Peak metamorphism, D$_2$ or correlative deformation, and associated syn-tectonic magmatism were dated between 430 and 420 Ma and hence formed during the Salinic orogeny (Dunning et al. 1990; Schofield et al. 1996; Schofield and D'Lemos 2000; Kellett et al. 2016). Steeply inclined or upright D$_3$ structures are syntectonic with Early Devonian granites (Schofield and D'Lemos 2000), whereas structures that equate with D$_2$ and D$_3$ herein were associated with sinistral shear zones (Holdsworth 1994; Schofield et al. 1996; Schofield and D'Lemos 2000; Kellett et al. 2016). Sinistral shear may have continued until the late Early Devonian (400–394 Ma) and replaced by more localized dextral shear by at least 385 Ma (Kellett et al. 2016). However, the evidence concerning the time of shear reversal is ambiguous on a regional scale such that a phase of Early Devonian localized dextral shear after the Silurian penetrative sinistral shear (Holdsworth 1994) is also compatible with the available data. The nearby Dog Bay Line, which separates the Gander margin from the rocks formed in the Exploits backarc basin (Figs 1 and 10A), accommodated Early Devonian dextral shear (Williams et al. 1993; Piasecki 1995). Hence the time when the switch from sinistral to dextral occurred regionally is not well defined and both dextral and sinistral shear may have overlapped in time in the various segments of the Gander margin. Dextral shear was prevalent during the Early Devonian D$_3$ in northcentral (Lafrance and Williams 1992) and southwest Newfoundland (Dubé and Lauzière 1996, this study), while sinistral shear may have continued during D$_3$ well into the Early Devonian in eastern Newfoundland. If dextral motion in the western parts of the Gander margin overlapped with sinistral in the east, it indicates that Ganderia was escaping southwards with respect to its bounding terranes.

Tectonic evolution of the Meelpaeg tectonites within the framework of Salinic and Acadian orogenesis in southern and northeastern Newfoundland

Salinic orogeny

The tectonic evolution of the Meelpaeg tectonites started when they were deeply buried following progressive Silurian underthrusting of elements of the Exploits backarc (GBC and PABC) and the Gander margin (HLCG) (Fig. 10A), beneath composite Laurentia. Correlative rocks such as the Bay du Nord, Red Cross, Bay d'Espoir, and underlying Gander groups (Fig. 1) were also involved in this tectonism, but equivalent deeply buried parts of these rocks are generally not exposed and probably still buried at depth as the Gander margin rocks have been traced seismically westwards to the base of the crust (van der Velden et al. 2004). Underthrusting of the Gander margin of the Exploits backarc basin followed the closure of the oceanic segment (van Staal 1994;

van Staal et al. 1998, 2014a, 2021; Valverde-Vaquero et al. 2006; Zagorevski et al. 2010), which was accompanied by a short lived (445–433 Ma) east-facing arc (Fig. 1) (Whalen et al. 2006) and a turbidite-rich forearc (Badger Group). The terminal Salinic suture is the Dog Bay Line (Williams et al. 1993; van Staal et al. 2014a), which separates the Gander margin rocks from volcano-sedimentary sequences that form part of the Victoria arc and Exploits backarc basin. The Dog Bay Line can be traced from northeastern Newfoundland into central Newfoundland (Valverde-Vaquero et al. 2006) and an allochthonous segment is preserved within the Meelpaeg structure as GRSZ (Fig. 10A). When the Salinic collision exactly started in southwestern Newfoundland is poorly constrained because the marine Indian Island foreland basin (Fig. 1) is not preserved here. However, it probably occurred earlier than further to the northeast, where it started at ca. 433 Ma (van Staal et al. 2014a) because it involved underthrusting by the Cabot promontory on the Gander margin (Lin et al. 1994; van Staal 1994; Valverde-Vaquero et al. 2006). In addition, some time is needed to structurally bury and metamorphose sedimentary rocks to upper amphibolite facies conditions at depths corresponding to ca. 10 Kb, even though the duration of the peak-temperature Barrovian metamorphism can be short-lived (Viete and Lister 2017). Marine sedimentation in the Salinic Badger forearc had ceased everywhere in Newfoundland at ca. 433 Ma (O'Brien 2003) and replaced by unconformable terrestrial red-bed sedimentation (e.g., Botwood Group) and associated magmatism, which become progressively younger eastwards (van Staal et al. 2014a). Ludlow red beds (ca. 422 Ma) overstepped the Dog Bay Line (Pollock et al. 2007) suggesting that the Salinic orogen was largely subaerial by this time, which is consistent with the Ludlow to Pridoli age (ca. 422 Ma) of the clastic-dominated Rocky Ridge belt (RRB in Fig. 1) of the Silurian La Poile Group (O'Brien et al. 1991). The RRB is lenticular and truncated by the Acadian dextral reverse Bay d'Est fault, which defines its northwestern boundary and separates it from the highly tectonized belts of the Bay du Nord Group to the north (Fig. 1), the southernmost belt of which (Dolman Cove belt of Tucker et al. 1994 and Chorlton and Dallmeyer 1986) contains coarse upper Silurian clastic rocks and interlayered tuff (Brian O'Brien (written communication, 2023)). The RRB has a significantly different stratigraphy compared to the remainder of the largely older Silurian volcanic-dominated La Poile Group, preserved further to the southwest from which it is isolated by faults (O'Brien et al. 1991, 1993). The stratigraphic linkage between the two separated belts of La Poile Group is represented by latest Silurian (ca. 422 Ma) felsic tuff interlayered with the clastic sedimentary rocks. The felsic tuff layers are coeval with the terminal felsic volcanic rocks in the La Poile Group proper (O'Brien et al. 1991); hence the RRB is largely younger. The predominance of Ludlow to Pridoli fluvial and alluvial coarse clastic rocks and conglomerate in the RRB and parts of the Dolman Cove belt suggest they may have formed part of a late Salinic molasse-type foreland cover deposited on the Gander margin in southwestern Newfoundland (van Staal et al. 2014a, 2021) inviting correlation with the coeval Botwood Group red beds that overstep the Dog Bay Line further to the northeast (Pollock et al. 2007).

Inversion of the molasse foredeep took place at ca. 419 Ma (O'Brien et al. 1991), which is interpreted as approximately dating the terminal stage of the Salinic collision in southwestern Newfoundland (Fig. 10A, stage B). This interpretation is consistent with the age constraints within error of D_{1-2} in the Meelpaeg structure, since D_2 terminated shortly after the early Lochkovian (ca. 417 Ma) intrusion of the large, late syntectonic Rose Blanche granite (Figs. 1 and 2). Formation of the Rose Blanche granite and associated migmatization, and other related coeval felsic and mafic magmatic rocks along strike, were related to melting induced by heat derived from the mantle following slab break-off and progressive opening and widening of an asthenospheric window beneath the Salinic orogen due to foreland migration of the trench of the A subduction zone (van Staal et al. 2014a; Figs. 8B and 8C). In this model, D_2 thus also includes deformation that overlapped with slab break-off. A comparable Salinic tectonic evolution was recognized elsewhere in central and southern Newfoundland (Valverde-Vaquero et al. 2006) and in correlative rocks in central New Brunswick, which show a surprisingly similar timeline of events (Wilson et al. 2017). The anomalous high grade of metamorphism compared to similar rocks along strike probably relates to prolonged underthrusting and structural thickening of buoyant continental Gander margin rocks of the Cabot promontory, whereas subduction of less-buoyant backarc lithosphere continued in the reentrants (van Staal 1994; Fig. 9). Slab break-off leads to rebound of the partially subducted buoyant slab (slab unbending of van Staal et al. 2014a; Fig. 8C), which is inferred to have progressively squeezed the deeply buried crustal rocks pulled down in the subduction channel and forced their movement upwards (van Agtmaal et al. 2022). Such southeast-directed upward flow of deeply buried high-grade rocks promoted tectonic escape (Fig. 10A, stage C), consistent with the monazite and titanite ages, suggesting the onset of retrograde amphibolite facies conditions and thus exhumation sometime between 417 and 412 Ma (Figs. 7 and 8). The lack of evidence for any west-directed tectonic transport, interpreted as the start of D_3, before 412 Ma suggests that southeast-directed tectonic transport of the Meelpaeg tectonictes continued in the period after slab break-off, which is consistent with tectonic escape. The deformation that accommodated tectonic escape had a similar style and sense of shear along its basal shear zone (Fig. 10A; stage C) as occurred during D_2 and D_3 in the eastern part of the Meelpaeg structure, hence would be difficult to recognise as a separate event. Three additional lines of evidence support the tectonic escape model: (1) deformation and mylonitization of the Rose Blanche granite in the BMFZ had started late during D_2 and continued after late syntectonic granite emplacement (Fig. 6B) and thus also peak Salinic metamorphism, (2) cooling and exhumation rates appear to be higher in the northwest than the southeast (Burgess et al. 1995), where the base of the inferred escaping wedge is located (Fig. 10A; stage C), and (3) offshoots of the 416 ± 4 Ma La Poile granite cut BMFZ and D_2 tectonites in the Rose Blanche granite further to the north (Fig. 1), but were subsequently deformed by D_3-related shearing and folding. Upwards flow of the buried rocks during the proposed tectonic escape demands the presence of normal sense shear

in the hanging wall of the escaping wedge (Fig. 10A, stage C) and shallow-to-moderate northwesterly dips in the GBC tectonites. The GBC tectonites now generally have a steep dip to the southeast between the CRFZ and the GBFZ (Figs. 2 and 9), which was established during the D_3 westwards-directed thrusting and subsequent F_3 folding (Fig. 10B, stage d). However, sinistral reverse shear sense indicators associated with southwest-plunging stretching lineations in amphibolite facies tectonites of the GBC, which predate the D_3-related dextral reverse movements and associated retrogressive metamorphism, adjacent to the CRFZ (Dubé and Lauzière 1996), are consistent with the tectonic escape model if the L-S fabric is restored to a pre-D_3 orientation characterized by northwestward dips. Such a restoration would produce a component of down–dip normal sense of shear associated with an early horizontal sinistral component in the CRFZ tectonites. A northwesterly dip of the D_{1-2} tectonites before D_3 is also consistent with the inferred southerly or southeasterly overturning and vergence of the F_2 folds after unfolding of F_3 in the IMDZ.

Acadian orogeny

The Acadian orogeny was attributed to the protracted Early Devonian collision of Avalonia (lower plate) with composite Laurentia (upper plate) that at this stage included all Ganderia (Fig. 10B) (Holdsworth 1994). A Silurian arc–backarc complex (coastal arc of van Staal and Barr 2012) was built on the southern edge of the Gander margin along the south coast of Newfoundland (Fig. 1) during closure of the Acadian seaway (van Staal et al. 2012). The Coastal Arc–backarc is represented by the Burgeo granite and coeval volcanic rocks of the La Poile Group (429–422 Ma, O'Brien et al. 1991) in southern Newfoundland (Fig. 1). However, the exact time when the Acadian seaway was closed, and Avalonia started to be underthrust beneath the Gander margin is uncertain in Newfoundland. The collision is generally thought to have started no later than 419 Ma, primarily based on the time of inversion of the La Poile backarc basin (van Staal and Barr 2012) and the onset of dextral oblique reverse movements (O'Brien et al. 1991, 1993). Acadian deformation propagated northwestwards in a retro-arc setting and lasted into the early Middle Devonian (Willner et al. 2018).

The evolution of the D_3 Acadian structures in the Meelpaeg structure is consistent with this tectonic model. Postcollision tectonic escape was shortly thereafter ($\leq$412 Ma) followed by Early Devonian Acadian bi-vergent oblique dextral reverse movements along the CRFZ and BMFZ early during D_3, which culminated in final emplacement of the Meelpaeg tectonites above the Windsor Point Group (terrestrial cover on Dashwoods) rocks to the west (Dubé et al. 1996; Dubé and Lauzière 1996), Devonian terrestrial sedimentary rocks of the Billiards Brook Formation to the northwest (Chorlton 1980), and Bay du Nord Group to the east (Figs. 1 and 10B; stages D and E). The sandstones of the Billiards Brook Formation (Figs. 1; BF) contain Emsian to Eifelian plant fossils (Chorlton 1980) and our investigations showed they were weakly folded and cleaved during overthrusting by the Victoria Lake shear zone in the northeastern reaches of the La Poile River (Fig. 1). The

Billiards Brook Formation is a correlative of a narrow belt of largely undeformed Lower Devonian terrestrial sedimentary rocks, which unconformably overlie Silurian red beds and Ordovician rocks of the Notre Dame arc, immediately west of the Beothuk Lake Line and Victoria Lake shear zone (Chandler 1982; van Staal et al. 2005). Where undeformed, the Devonian terrestrial rocks define the Acadian deformation front in central Newfoundland (van Staal and Zagorevski 2017; Willner et al. 2018). Progressive retrogression in the metamorphic tectonites of the GBC and PABC where overprinted by D_3 shear zones is recorded by microstructures (see above) and Early Devonian titanite and Ar ages (Figs. 2 and 8), which attest to continuous exhumation of these rocks during the Acadian oblique reverse and dextral strike–slip movements, and F_3 folding. Hence, D_3 must have been accompanied by significant denudation, the products of which are probably preserved in the Early Devonian molasse basins that are preserved in the belt of terrestrial Devonian rocks immediately west of the Beothuk Lake Line and along the southeast coast of Newfoundland in the Lower to Upper Devonian red beds of the Fortune belt (Fig. 10A and 10B, Williams and O'Brien 1995; van Staal et al. 2014*b*) near Belleoram, immediately southeast of the Dover–Hermitage fault that separates the Gander margin from Avalonia (Fig. 1).

Promontory collision and formation of the meelpaeg structure

Southwestern Newfoundland and nearby Cape Breton Island (Lin and van Staal 1997; Lin 2001) preserve allochthonous Salinic to Acadian amphibolite facies metamorphic tectonites, which are notably absent along strike elsewhere in the Canadian and adjacent northern New England Appalachians. This structural style coincides with the outlines of promontories on the margins of Laurentia (St. Lawrence promontory) and Ganderia (Cabot promontory) in the Canadian Appalachians (Williams 1979) and were attributed by Lin et al. (1994) and van Staal (1994) to a promontory–promontory collision. Prolonged underthrusting of the Cabot promontory beneath composite Laurentia probably caused enhanced Salinic structural thickening and exhumation compared to the collisional wedge along strike in the adjacent reentrants. This inference is supported by thermomechanical models (Koptev et al. 2019), which suggest that uplift and exhumation rates are rapid and more pronounced in areas where promontories are involved in collision.

Do Salinic and Acadian orogenies represent one continuous orogenic cycle or two separate kinematic events?

Separation of Salinic and Acadian structures in Newfoundland and the northern Appalachians in general is problematic, since both orogenic cycles were diachronous, and may have overlapped in time (van Staal et al. 2014*a*). The age constraints presented herein for the structural evolution of the infra-structure of the Salinic and Acadian orogen of south-

western Newfoundland highlight this problem since there is little or no time gap between the end of the Salinic (419–417 Ma) and post-collision deformation associated with the inferred tectonic escape (417–412 Ma) (Figs. 8 and 10*a*), and the onset of the Acadian (≤412 Ma). Hence, one could argue that Silurian Salinic orogenesis seamlessly transitioned into Early Devonian Acadian orogenesis supporting the arguments of earlier workers who argued they represent one continuous event based on classifying orogenies solely on time (e.g., Murphy and Keppie 2005). If so, deformation of the tectonites in the Meelpaeg structure should be driven by a continuing collision between the Gander margin and composite Laurentia into the Devonian. In such a scenario, the west-directed CRFZ should represent a major retroshear (Fig. 10B). However, thermo-mechanical modelling shows that retroshears and doubly vergent orogens typically develop during prolonged subduction of relatively wide oceanic basins with considerable slab pull, whereas closure of narrow basins such as the Tetagouche–Exploits backarc (≤800 km, van Staal et al. 2012) typically produces single vergent orogenic wedges, slab detachment at shallow levels causing tectonic escape of partially subducted continental crust, and an asthenospheric window beneath the orogen (van Agtmaal et al. 2022), which correspond better with the observed characteristics associated with the Salinic orogen (van Staal et al. 2014*a*; Wilson et al. 2017). Hence, we do not support a kinematically continuous ca. 70 my Salinic–Acadian orogenic cycle. Particularly, the Silurian to Devonian arc magmatism on the Gander margin (van Staal and Barr 2012) supports the presence of Acadian subduction independent of the convergence responsible for the Salinic orogenesis (Fig. 10B). In addition, Early Devonian dextral oblique movements are typically associated with Acadian structures in the central part of the northern Appalachians (e.g., Lafrance and Williams 1992; Hibbard 1994; van Staal and de Roo 1995; Dubé et al. 1996), whereas the Salinic orogeny in Newfoundland is generally characterized by wide Salinic sinistral shear zones in the Gander margin, which suggest that the obliquity of the responsible Salinic convergence was sinistral rather than dextral (Hanmer 1981; O'Brien et al. 1993; Holdsworth 1994; Piasecki 1995; Kellet et al. 2016). Hence the switch from sinistral to dextral oblique convergence during the Early Devonian as observed in southwestern Newfoundland is potentially a tool to separate structures formed during the Salinic and Acadian orogenies in the central part of the northern Appalachians. However, as discussed above evidence suggests that there may have been coeval sinistral and dextral motions along each side of the Gander margin for some time, particularly since dextral shear may have started at the end of Rose Blanche magmatism in mylonites of the BMFZ (Fig. 6B), thus potentially being active during the inferred post-collision tectonic escape. The duration of the various strike–slip motions and when the Acadian collision exactly started is still unresolved. Inversion of the La Poile basin at ca. 419 Ma (O'Brien et al. 1991), previously inferred to mark the onset of the Acadian collision (van Staal and Barr 2012), may be a terminal Salinic (Fig. 8) rather than an Acadian-related phenomenon consistent with the oldest-known Acadian foreland basin clastic rocks on Avalonia in southern Newfoundland, which are not older than Early De-

vonian (Fortune belt of Williams and O'Brien 1995; van Staal et al. 2014*b*). An Early Devonian start of the Acadian orogeny would avoid overlap in time between the last gasps of the Salinic and onset of the Acadian. Alternatively, start of the Acadian collision between Avalonia and the adjacent Gander margin near the Silurian–Devonian boundary (ca. 419 Ma) may have instigated the change in oblique convergence due to subduction stepping back into the Rheic Ocean outboard of Avalonia and producing dextral oblique convergence in the upper plate (composite Laurentia of van Staal and Barr 2012) early in the Devonian. Regardless, the bulk of the Acadian orogeny in the central core of the northern Appalachians was associated with dextral kinematics during the Early Devonian. Hence, the kinematic switch from sinistral to dextral between Salinic and most Acadian structures in this part of the orogen supports a separation in two different orogenies, rather than combining them into one long-lasting orogeny (Murphy and Keppie 2005).

Article information

Notes

This paper is part of a collection in honour of Dr. Nick Culshaw entitled "From Outcrops to Orogens: A Celebration of the Career of Nick Culshaw".

Copyright

Data availability

Thin sections used for microstructural analysis and rocks used for dating are available at the Geological Survey of Canada and Memorial University of Newfoundland.

Author information

Author ORCIDs

C. R. van Staal https://orcid.org/0000-0003-2232-0577

Author contributions

Conceptualization: CRvS
Data curation: CRvS, SL, PV, GD, JB, DS, NJ
Formal analysis: CRvS, SL, PV, GD, JB, DS, NJ
Funding acquisition: CRvS
Investigation: CRvS, SL, PV, GD, JB, DS, NJ
Methodology: CRvS, SL, PV, GD, JB, DS, NJ
Project administration: CRvS
Resources: CRvS, PV, GD, JB
Software: PV, GD, NJ
Supervision: CRvS
Validation: CRvS, SL, PV, GD, JB, DS, NJ
Visualization: CRvS, PV, NJ
Writing – original draft: CRvS
Writing – review & editing: CRvS, SL, PV, GD, JB, DS, NJ

Competing interests

No competing interests.

References

Bagherpur Mojaver, O., Darbyshire, F., and Dave, R. 2021. Lithospheric structure and flat-slab subduction in the northern Appalachians: evidence from Rayleigh wave tomography. Journal of Geophysical Research: Solid Earth, **126**(4): e2020JB020924. doi:10.1029/2020JB020924.

Benn, K, Genkin, M., and van Staal, C.R. 1993. Structure and anisotropy of magnetic susceptibility of the Rose Blanche Granite, southwestern Newfoundland: kinematics and relative timing of emplacement. In Current Research, Part D, Geological Survey of Canada, Paper **93-1D**. pp. 73–82.

Blackwood, R.F. 1983. Geology of the Facheux Bay map area (11P/9), southern Newfoundland. In Current research. Newfoundland Department of Mines and Energy, Mineral Development Division, Report 83-1. pp. 26–40.

Blackwood, R.F. 1984. Geology of the west half of the Dolland Brook map area (11P/15), southern Newfoundland. In Current research. Newfoundland Department of Mines and Energy, Mineral Development Division, Report 84-1. pp. 198–209.

Blackwood, R.F. 1985. Geology of the Facheux Bay area (11P/9), Newfoundland. Department of Mines and Energy, Government of Newfoundland and Labrador Report **85-4**. 56p.

Bradley, D.C., Tucker, R.D., Lux, D.R., Harris, A.G., and McGregor, D.C. 2000, Migration of the Acadian Orogen and foreland basin across the northern Appalachians of Maine and adjacent areas. United States Geological Survey Professional Paper **1624**. 49 p.

Brown, P.A. 1976. Geology of the Rose Blanche map-area (110/11), Newfoundland. Newfoundland Department of Mines and Energy, Mineral Development Division, Report **76-5**. 16 p.

Burgess, J.L., Brown, M., Dallmeyer, R.D., and van Staal, C.R. 1995. Microstructure, metamorphism, thermochronology and P-T-t deformation history of the Port aux Basques gneisses, south-west Newfoundland, Canada. Journal of Metamorphic Geology, **13**: 751–776. doi:10.1111/j.1525-1314.1995.tb00257.x.

Chandler, F.W. 1982. Sedimentology of two Middle Paleozoic terrestrial sequences, King George IV Lake area. In Current Research, Part B. Geological Survey of Canada Paper 82-1A. pp. 213–219.

Chorlton, L.B. 1980. Geology of the La Poile River area (110/16), Newfoundland. Department of Mines and Energy, Government of Newfoundland and Labrador Report 80-3. 86p.

Chorlton, L.B., and Dallmeyer, R.D. 1986. Geochronology of Early to middle Paleozoic tectonic development in the southwest Newfoundland Gander Zone. The Journal of Geology, **94**: 67–89. doi:10.1086/629010.

Cohen, K.M., Finney, S.C., Gibbard, P.L., and Fan, J.-X. 2022. The ICS International Chronostratigraphic Chart. Episodes, **36**: 199–204. http://www.stratigraphy.org/ICSchart/ChronostratChart2022-02.pdf. doi:10.18814/epiiugs/2013/v36i3/002.

Colman-Sadd, S.P. 1980. Geology of south-central Newfoundland and evolution of the eastern margin of Iapetus. American Journal of Science, **280**: 991–1017. doi:10.2475/ajs.280.10.991.

Colman-Sadd, S.P., Dunning, G.R., and Dec, T. 1992. Dunnage–Gander relationships and Ordovician orogeny in central Newfoundland: a sediment provenance and U/Pb study. American Journal of Science, **292**: 317–355. doi:10.2475/ajs.292.5.317.

Colman-Sadd, S.P., Hayes, J.P., and Knight, I. 1990. Geology of the Island of Newfoundland. Newfoundland Department of Mines and Energy, Geological Survey Branch, Map 90-01.

Dokken, R.J., Waldron, J.W.F., and Dufrane, A. 2018. Detrital zircon geochronology of the Fredericton Trough, New Brunswick, Canada: constraints on the Silurian closure of remnant Iapetus Ocean. American Journal of Science, **318**: 684–725. doi:10.2475/06.2018.03.

Dubé, B., and Lauzière, K. 1996. Structural evolution of a major fault zone: the Cape Ray Fault Zone, southwestern Newfoundland, Canada. Canadian Journal of Earth Sciences, **33**: 199–215. doi:10.1139/e96-018.

Dubé, B., Dunning, G.R., Lauzie`re, K., and Roddick, J.C. 1996. New insights into the Appalachian Orogen from geology and geochronology along the Cape Ray fault zone, southwest Newfoundland. Geological Society of America Bulletin, **108**: 101–116. doi:10.1130/0016-7606(1996)108⟨0101:NIITAO⟩2.3.CO;2.

Dunning, G, O'Brien, S.J., Colman-Sadd, S.P., Blackwood, R., Dickson, WL, O'Neill, P.P., and Krogh, T.E. 1990. Silurian orogeny in the Newfoundland Appalachians. The Journal of Geology, **98**: 895–913. doi:10.1086/629460.

Eusden, J. D, Hillenbrand, I.W., Folsom, E., Merril, T, Niiler, K., and Wheatcroft, A. 2023. Evolution of the Bronson Hill arc and Central Maine basin, northern New Hampshire to western Maine: U-Pb zircon constraints on the timing of magmatism, sedimentation and tectonism. In Laurentia: turning points in the evolution of a continent: Geological Society of America Memoir. Vol. 220. Edited by S.J. Whitmeyer, M.L. Williams, D.A. Kellett and B. Tikoff. Geological Society of America, Boulder, CO. pp. 533–560. doi:10.1130/2022.1220(26).

Fyffe, L.R., van Staal, C.R., Wilson, R.A., and Johnson, S.C. 2023. An overview of early Paleozoic arc systems in New Brunswick, Canada and eastern Maine, USA. Atlantic Geoscience, **59**: 01–028. doi:10.4138/atlgeo.2023.001.

Hanmer, S. 1981. Tectonic significance of the Gander Zone, Newfoundland: an Acadian ductile shear zone. Canadian Journal of Earth Sciences, **18**: 120–135. doi:10.1139/e81-010.

Hanmer, S. 1988. Ductile thrusting at mid-crustal level, southwestern Grenville province. Canadian Journal of Earth Sciences, **25**: 1049–1059. doi:10.1139/e88-102.

Hartnady, M.I.H., Kirkland, C.L., Clark, C., Spaggiari, C.V., Smithies, R.H., Evans, N.J., and McDonald, B.J. 2019. Titanite dates crystallization: slow Pb-diffusion during super-solidus re-equilibration. Journal of Metamorphic Geology, **37**: 823–838. doi:10.1111/jmg.12489.

Hibbard, J. 1994. Kinematics of the Acadian deformation in the Northern and Newfoundland Appalachians. The Journal of Geology, **102**: 215–228. doi:10.1086/629664.

Hibbard, J., van Staal, C.R., Rankin, D., and Williams, H. 2006. Geology, Lithotectonic map of the Appalachian Orogen, Canada—United States of America. Geological Survey of Canada, Map 2096A, scale 1:1 500 000.

Hillenbrand, I.W., Williams, M.L., Li, C., and Gao, H. 2021. Rise and fall of the Acadian altiplano: evidence for a Paleozoic orogenic plateau in New England. Earth and Planetary Science Letters, **560**: 116797. doi:10.1016/j.epsl.2021.116797.

Holdsworth, R.E. 1994. Structural evolution of the Gander–Avalon terrane boundary: a reactivated transpression zone in the NE Newfoundland Appalachians. Journal of the Geological Society, **151**: 629–646. doi:10.1144/gsjgs.151.4.0629.

Honsberger, I.W., Bleeker, W., Kamo, S.L., Sandeman, H.A.I., Evans, D.T.W., Rogers, N., et al. 2022. Latest Silurian syntectonic sedimentation and magmatism and Early Devonian orogenic gold mineralization, central Newfoundland, Canada: structure, lithogeochemistry, and high-precision U–Pb geochronology. GSA Bulletin, **134**: 2933–2957. doi:10.1130/B36083.1.

Kellett, D.A., Warren, C., Larson, K.P., Zwingmann, H., van Staal, C.R., and Rogers, N. 2016. Influence of deformation and fluids on Ar retention in white mica: dating the Dover fault, Newfoundland, Appalachians. Lithos, **254-255**: 1–17. doi:10.1016/j.lithos.2016.03.003.

Kerr, A., van Nostrand, T.S., Dickson, W.L., and Lynch, E.P. 2009. Molybdenum and tungsten in Newfoundland: a geological overview and summary of recent exploration developments. Current Research, Newfoundland and Labrador Department of Natural Resources Geological Survey, Report **09-1**. pp. 43-80.

Koptev, A., Ehlers, T.A., Nettesheim, M., and Whipp, D.M. 2019. Response of a rheologically stratified lithosphere to subduction of an indenter-shaped plate: insights into localized exhumation at orogen syntaxes. Tectonics, **38**: 1908–1930. doi:10.1029/2018TC005455.

Krogh, T.E. 1982. Improved accuracy of U–Pb zircon ages by the creation of more concordant systems using an air abrasion technique. Geochimica et Cosmochimica Acta, **46**: 637–649. doi:10.1016/0016-7037(82)90165-X.

Lafrance, B., and Williams, P.F. 1992, Silurian deformation in eastern Notre Dame Bay, Newfoundland. Canadian Journal of Earth Sciences, **29**: 1899–1914. doi:10.1139/e92-148.

Lin, S. 2001. ^{40}Ar/^{39}Ar age pattern associated with differential uplift along the Eastern Highlands shear zone, Cape Breton Island, Canadian Appalachians. Journal of Structural Geology, **23**: 1031–1042. doi:10.1016/S0191-8141(00)00174-7.

Lin, S., and van Staal, C.R. 1997. Comment on "Tectonic burial, thrust emplacement, and extensional exhumation of the Cabot nappe in the Appalachian hinterland of Cape Breton Island, Canada" by G. Lynch. Tectonics, **16**: 702–706. doi:10.1029/97TC01088.

Lin, S., van Staal, C.R., and Dubé, B. 1994. Promontory-promontory collision in the Canadian Appalachians. Geology, **22**: 897–900. doi:10.1130/0091-7613(1994)022%3c0897:PPCITC%3e2.3.CO;2.

Lin, S., van Staal, C.R., and Lee, C. 1993. The Harbour Le Cou Group and its correlation with the Bay du Nord Group, southwestern Newfoundland. In Current Research, Part D, Geological Survey of Canada, Paper 93-1D. pp. 57-64.

Ludwig, K.R. 1999. Isoplot/Ex Version 2.00: a Geochronological Toolkit for Microsoft Excel. Berkeley Geochronology Center Special Publications, 1a.

Martin, A.J., Gehrels, G.E., and de Celles, P.G. 2007. Tectonic significance of (U,Th)/Pb ages of monazite inclusions in garnet from the Himalaya of central Nepal. Chemical Geology, **244**: 1–24. doi:10.1016/j.chemgeo.2007.05.003.

Murphy, J.B., and Keppie, J.D. 2005. The Acadian orogeny in the Northern Appalachians. International Geology Review, **47**: 663–687. doi:10.2747/0020-6814.47.7.663.

O'Brien, B. 2003. Geology of the central Notre Dame Bay region (parts of NTS areas 2E/3,6,11), northeastern Newfoundland. Government of Newfoundland and Labrador Department of Mines and Energy, Report 03-03, 147 p.

O'Brien, B.H. 1987. The lithostratigraphy and structure of the Grand Bruit-Cinq Cerf area (parts of NTS areas 11O/9 and 11O/16), southwestern Newfoundland. Current Research, newfoundland Department of

mines and Energy, Mineral Development Division, Report **87-1**. pp. 311–334.

O'Brien, B.H. 1988. The relationships of phyllite, schist and gneiss in the La Poile-Roti Bay area (parts of NTS areas 11O/9 and 11O/16), southwestern Newfoundland. Current Research, newfoundland Department of mines and Energy, Mineral Development Division, Report **88-1**. pp. 109–125.

O'Brien, B.H., O'Brien, S.J., and Dunning, G.R. 1991. Silurian cover, Late Precambrian-Early Ordovician basement, and the chronology of Silurian orogenesis in the Hermitage Flexure (Newfoundland Appalachians. American Journal of Science, **291**: 760–799. doi:10.2475/ajs.291.8.760.

O'Brien, B.H., O'Brien, S.J., Dunning, G.R., and Tucker, R.D. 1993. Episodic reactivation of a Late Precambrian mylonite zone on the Gondwanan margin of the Appalachians, southern Newfoundland. Tectonics, **12**: 1043–1055. doi:10.1029/93TC00110.

Owen, J.V. 1992. Comparative petrology of gneissic rocks in southwestern Newfoundland. Canadian Journal of Earth Sciences, **29**: 2663–2676. doi:10.1139/e92-211.

Passchier, C.W., and Trouw, R.A.J. 2005. Microtectonics. 2nd revised ed. Springer, Berlin. 366p.

Piasecki, M.A.J., 1995. Dunnage zone boundaries and some aspects of terrane development in Newfoundland. In Current perspectives in the Appalachian–Caledonian Orogen. Edited by J. Hibbard, C.R. van Staal and P. Cawood. Geological Association of Canada Special PaperNo. **41**. pp. 323–347.

Pollock, J.C., Wilton, D.H.C., van Staal, C.R., and Morrissey, K.D. 2007. U–Pb detrital zircon geochronological constraints on the early Silurian collision of Ganderia and Laurentia along the Dog Bay Line: the terminal Iapetan suture in the Newfoundland Appalachians. American Journal of Science, **307**: 399–433. doi:10.2475/02.2007.04.

Ramsay, J.G. 1967. Folding and fracturing of rocks, McGraw-Hill, Inc., New York, NY. 568p.

Reusch, D., and van Staal, C.R. 2012. The Dog Bay-Liberty Line and its significance for Silurian tectonics of the northern Appalachian orogen. Canadian Journal of Earth Sciences, **49**: 239–258. doi:10.1139/e11-024.

Rogers, N., van Staal, C.R., McNicoll, V., Pollock, J., Zagorevski, A., and Whalen, J. 2006. Neoproterozoic and Cambrian arc magmatism along the eastern margin of the Victoria Lake Supergroup: a remnant of Ganderian basement in central Newfoundland? Precambrian Research, **147**: 320–341. doi:10.1016/j.precamres.2006.01.025.

Schofield, D., D'Lemos, R., and King, T. 1996. Evidence and implications for the syn-tectonic emplacement of the Cape Freels Granite: a Silurian pluton emplaced into the Gander Lake Subzone, northeast Newfoundland. In Current research. Newfoundland Department of Natural Resources, Geological Survey, Report 96-1, pp. 329–342.

Schofield, D., van Staal, C.R., and Winchester, J. 1998. Tectonic setting and regional significance of the Port aux Basques Gneiss, SW Newfoundland. Journal of the Geological Society, **155**: 323–334. doi:10.1144/gsjgs.155.2.0323.

Schofield, D.I., and D'Lemos, R.S. 2000, Granite petrogenesis in the Gander Zone, NE Newfoundland: mixing of melts from multiple sources and the role of lithospheric delamination. Canadian Journal of Earth Sciences, **37**: 535–547. doi:10.1139/e99-116.

Slack, J.F., Swinden, H.S., Piercey, S.L., Ayuso, R.A., van Staal, C.R., and LeHurray, A.P. 2024. Lead isotopes in New England (USA) volcanogenic massive sulfide deposits: implications for metal sources and pre-accretionary tectonostratigraphic terranes. Canadian Journal of Earth Sciences, **6**: 1–16. doi:10.1139/cjes-2023-0058.

Thurlow, J.G., Spencer, C.P., Boerner, D.E., Reed, L.E., and Wright, J.A. 1992, Geological interpretation of a high resolution seismic survey at the Buchans mine, Newfoundland. Canadian Journal of Earth Sciences, **29**: 2022–2037. doi:10.1139/e92-159.

Tucker, R.D., O'Brien, S.J., and O'Brien, B.H. 1994. Age and implications 0f Early Ordovician (Arenig) plutonism in the type area of the Bay du Nord Group, Dunnage Zone, southern Newfoundland Appalachians. Canadian Journal of Earth Sciences, **31**: 351–357. doi:10.1139/e94-032.

Valverde-Vaquero, P., Dunning, G, and van Staal, C.R. 2000. The Margaree orthogneiss (Port aux Basques Complex, SW Newfoundland) evolution of a peri-Gondwanan, Mid Arenig-Early Llanvirn, mafic-felsic

igneous complex. Canadian Journal of Earth Sciences, **37**: 1691–1710. doi:10.1139/e00-053.

Valverde-Vaquero, P., van Staal, C.R., McNicoll, V., and Dunning, G. 2006. Middle Ordovician magmatism and metamorphism along the Gander margin in Central Newfoundland. Journal of the Geological Society, **163**: 347–362. doi:10.1144/0016-764904-130.

van Agtmaal, L., van Dinther, Y., Willingshofer, E., and Matenco, L. 2022. Quantifying continental collision dynamics for Alpine-style orogens. Frontiers in Earth Science, **10**: 916189. doi:10.3389/feart.2022.916189.

van der Velden, A.J., van Staal, C.R., and Cook, F.A. 2004. Crustal structure, fossil subduction and the tectonic evolution of the Newfoundland Appalachians: evidence from a reprocessed seismic reflection survey. Geological Society of America Bulletin, **116**: 1485–1498. doi:10.1130/B25518.1.

van Staal, C.R. 1994. The Brunswick subduction complex in the Canadian Appalachians: record of the Late Ordovician to Late Silurian collision between Laurentia and the Gander margin of Avalon. Tectonics, **13**: 946–962. doi:10.1029/93TC03604.

van Staal, C.R., and Barr, S.M. 2012. Lithospheric architecture and tectonic evolution of the Canadian Appalachians and associated Atlantic margin. Chapter 2. *In* Tectonic Styles in Canada: the Lithoprobe perspective. *Edited by* J.A. Percival, F.A. Cook and R.M. Clowes. Geological Association of Canada Special PaperNo. **49**. pp. Geological Association of Canada, St. John's, NL. 41–95.

van Staal, C.R., and de Roo, J.A. 1995. Mid-Paleozoic tectonic evolution of the Appalachian Central Mobile Belt in northern New Brunswick, Canada: collision, extensional collapse, and dextral transpression. *In* Current perspectives in the Appalachian–Caledonian Orogen. *Edited by* J. Hibbard, C.R. van Staal and P. Cawood. Geological Association of Canada Special Paper **41**. Geological Association of Canada, St. John's, NL. pp. 367–389.

van Staal, C.R., and Zagorevski, A. 2017. Accreted terranes of the Appalachian Orogen in Central Newfoundland. Geological Association of Canada. Mineralogical Association of Canada. Joint Annual Meeting. Field Trip Guidebook. 97 p.

van Staal, C.R., Barr, S.M., and Murphy, J.B. 2012. Provenance and tectonic evolution of Ganderia: constraints on the evolution of the Iapetus and Rheic oceans. Geology, **40**: 987–990. doi:10.1130/G33302.1.

van Staal, C.R., Barr, S.M., Waldron, J.W.F., Schofield, D.I., Zagorevski, A., and White, C.E. 2021. Provenance and Paleozoic tectonic evolution of Ganderia and its relationships with Avalonia and Megumia in the Appalachian-Caledonide orogeny. Gondwana Research, **98**: 212–243. doi:10.1016/j.gr.2021.05.025.

van Staal, C.R., Currie, K.L., Rowbotham, G., Goodfellow, W., and Rogers, N. 2008. P-T paths and exhumation of Late Ordovician-Early Silurian blueschists and associated metamorphic nappes of the Salinic Brunswick subduction complex, northern Appalachians. Geological Society of America Bulletin, **120**: 1455–1477. doi:10.1130/B26324.1.

van Staal, C.R., Dewey, J.F., MacNiocaill, C., and McKerrow, W.S. 1998. The Cambrian-Silurian tectonic evolution of the Northern Appalachians and British Caledonides: history of a complex, west and southwest Pacific-type segment of Iapetus. In Lyell, The past is the key to the present. *Edited by* D.J. Blundell and A.C. Scott. Geological Society of London, Special Publication No. **143**. Geological Society of London, London. pp. 199–242.

van Staal, C.R., Hall, L., Scofield, D., and Valverde, P. 1996a. Geology Port aux Basques, Newfoundland (part of NTS 11-O/11): Geological Survey of Canada, Open File 3165, scale 1: 25 000.

van Staal, C.R., Lin, S., Hall, L., Valverde, P., and Genkin, M. 1996b. Geology Rose Blanche, Newfoundland (NTS 11-O/10); Geological Survey of Canada, Open File 3219, scale 1: 25 000.

van Staal, C.R., Valverde-Vaquero, P., Zagorevski, A, Boutsma, S., Pehrsson, S., van Noorden, M., and McNicoll, V. 2005. Geology, King George IV Lake, Newfoundland (NTS 12-A/04): Geological Survey of Canada, Open File OF1665, scale 1:50,000, 1 sheet.

van Staal, C.R., Whalen, J.B., McNicoll, V.J., Pehrsson, S.J., Lissenberg, C.J., Zagorevski, A., et al. 2007. The Notre Dame arc and the Taconic orogeny in Newfoundland. *In* Catalán eds, 4-D framework of continental crust, *Edited by* Hatcher Jr., M.P. Carlson, J.H. McBride and J.R. Martínez. Geological Society of America, Boulder, CO. pp. 511–552.

Van Staal, C.R., Wilson, R.A., Kamo, S.L., McClelland, W.C., and McNicoll, V. 2016. Evolution of the Early to Middle Ordovician Popelogan arc in New Brunswick, Canada and Maine, USA: record of arc-trench migration and multiple phases of rifting. Geological Society of America Bulletin, **128**: 122–146. doi:10.1130/B31253.1.

Van Staal, C.R., Wilson, R.A., Rogers, N., Fyffe, L.R., Langton, J.P., McCutcheon, S.R., et al. 2003. Geology and tectonic history of the Bathurst Supergroup and its relationships to coeval rocks in southwestern New Brunswick and adjacent Maine—a synthesis. *In* Massive sulfide deposits of the Bathurst Mining Camp, New Brunswick, and Northern Maine, Economic Geology Monograph. Vol. 11. *Edited by* W.D. Goodfellow, S.R. McCutcheon and J.M. Peter. Society of Economic Geologists, Littleton, CO. pp. 37–60.

van Staal, C.R., Winchester, J.A., Brown, M., and Burgess, J.L. 1992. A reconaissance geotraverse through southwestern Newfoundland. In Current Research, Part D, Geological Survey of Canada Paper **92-1D**. pp. 133–144.

van Staal, C.R., Zagorevski, A., McNicoll, V., and Rogers, N. 2014a. The time transgressive Salinic and Acadian orogenesis, magmatism and old red sandstone sedimentation in Newfoundland. Geoscience Canada, **41**: 138–164. doi:10.12789/geocanj.2014.41.031.

van Staal, C.R., Ruberti, G., Kerr, A., and Conliffe, J. 2014b. The coast of bays: Paleozoic tectonic evolution of the Gander margin and adjacent Avalonia in southwestern Newfoundland. Geological Association of Canada, Newfoundland and Labrador section 2014 fall field trip. 42p.

Viete, D.R., and Lister, G.A. 2017. On the significance of short-duration regional metamorphism. Journal of the Geological Society, **174**: 377–392. doi:10.1144/jgs2016-060.

Waldron, J.W. F, McCausland, P.J.A., Barr, S.M., Schofield, D.I., Reusch, D., and Wu, L. 2022. Terrane history of the Iapetus Ocean as preserved in the northern Appalachians and western Caledonides. Earth-Science Reviews, **233**: 104163. doi:10.1016/j.earscirev.2022.104163.

Whalen, J.B., McNicoll, V.J., van Staal, C.R., Lissenberg, C.J., Longstaffe, F.J., Jenner, G.A., and van Breemen, O. 2006. Spatial, temporal, and geochemical characteristics of Silurian collision-zone magmatism: an example of a rapidly evolving magmatic system related to slab break-off. Lithos, **89**: 377–404. doi:10.1016/j.lithos.2005.12.011.

Whalen, J.B., van Staal, C.R., Longstaffe, F.J., Gariepy, C., and Jenner, G.A. 1997. Insights into tectonostratigraphic zone identification in southwestern Newfoundland based on isotopic (Nd, O, Pb) and geochemical data. Atlantic Geology, **33**: 231–241. doi:10.4138/2071.

Williams, H. 1979. Appalachian Orogen in Canada. Canadian Journal of Earth Sciences, **16**: 792–807. doi:10.1139/e79-070.

Williams, H., and O'Brien, S.J. 1995. Fortune belt, *In* Geology of the Appalachian–Caledonian Orogen in Canada and Greenland. Geology of Canada Series, No. 6. *Edited by* H. Williams. Geological Survey of Canada, Ottawa, ON. pp. 423–425. doi:10.4095/205242.

Williams, H., Colman-Sadd, S.P., and Swinden, H.S. 1988. Tectonic-stratigraphic subdivisions of central Newfoundland. Geological Survey of Canada Paper, **88-1B**: 91–98.

Williams, H., Currie, K.L., and Piasecki, M.A.J. 1993. The Dog Bay Line; a major Silurian tectonic boundary in Northeast Newfoundland. Canadian Journal of Earth Sciences, **30**: 2481–2494. doi:10.1139/e93-215.

Williams, P.F., Means, W.D., and Hobbs, B.E. 1977. Development of axial-plane slaty cleavage and schistosity in experimental and natural materials. Tectonophysics, **42**: 139–158. doi:10.1016/0040-1951(77)90165-2.

Willner, A.P., van Staal, C.R., Zagorevski, A., Glodny, J., Romer, R.L., and Sudo, M. 2018. Tectono-metamorphic evolution along the Iapetus suture zone in Newfoundland: evidence for polyphase Salinic, Acadian and Neoacadian very low- to medium-grade metamorphism and deformation. Tectonophysics, **742-743**: 137–167. doi:10.1016/j.tecto.2018.05.023.

Wilson, R.A., van Staal, C.R., and Kamo, S.L. 2017. Rapid transition from the Salinic to Acadian orogenic cycles in the northern Appalachian Orogen: evidence from northern New Brunswick, Canada. American Journal of Science, **317**: 449–482. doi:10.2475/04.2017.02.

Wilson, R.A., van Staal, C.R., and McClelland, W.C. 2015. Synaccretionary sedimentary and volcanic rocks in the Ordovician Tetagouche backarc basin, New Brunswick, Canada: evidence for a transition from foredeep to forearc basin sedimentation. American Journal of Science, **315**: 958–1001. doi:10.2475/10.2015.03.

Zagorevski, A., van Staal, C.R., and Joyce, N. 2024. The provenance and tectonic history of Dashwoods and the associated Baie Verte Margin during the Ordovician to Silurian. *In* Supercontinents, orogenesis and magmatism, *Edited by* R.D. Nance, R.A. Strachan, C. Quesada and S. Lin. Geological Society, London. doi:10.1144/sp542-2023-20.

Zagorevski, A., van Staal, C.R., and McNicoll, V.J. 2007. Distinct Taconic, Salinic, and Acadian deformation along the Iapetus suture zone, Newfoundland Appalachians. Canadian Journal of Earth Sciences, **44**: 1567–1585. doi:10.1139/e07-037.

Zagorevski, A., van Staal, C.R., McNicoll, V., Rogers, N., and Valverde-Vaquero, P. 2008. Tectonic architecture of an arc–arc collision zone, Newfoundland Appalachians. *In* Formation, and applications of the sedimentary record in arc-collision zones, *Edited by* A. Draut, P. Clift and D. Scholl. Geological Society of America, Ottawa, ON. 309–334.

Zagorevski, A., van Staal, C.R., Rogers, N., McNicoll, V., Dunning, G.R., and Pollock, J.C. 2010. Middle Cambrian to Ordovician arc-backarc development on the leading edge of Ganderia, Newfoundland Appalachians. Geological Society of America Memoir, **206**: 367–396.